

# Synthesis, Characterization, Computational, DNA Binding and Cleavage Studies of Cu (II), Co (II), and Ni (II) Metal Complexes Derived N'-(E)-(3-hydroxynaphthalen-2-yl) methylidene] pyridine-4-carbohydrazide

Ereshanaik<sup>1</sup>; M. C. Prabhakara<sup>1\*</sup>; Nagendra Naik K.<sup>2</sup>; Raghavendra S. M.<sup>1</sup>; Surendranai Y.<sup>3</sup>

<sup>1</sup>Department of PG Studies and Research in Industrial Chemistry, Sir. M.V. Govt. Science College, Bommanakatte, Bhadravathi, 577 302, Karnataka, India

<sup>2</sup>Department of Environmental Science, Government First Grade College, Davanagere – 577004, Karnataka, India

<sup>3</sup>Department of PG Studies and Research in Chemistry, Jnana Sahyadri, Kuvempu University, Shankaragatta, 577 451, Karnataka, India

Corresponding Author: M. C. Prabhakara<sup>1\*</sup>

Publication Date: 2026/02/14

**Abstract:** We describe the synthesis, detailed characterization, and biological assessment of new Cu (II), Co (II), and Ni (II) complexes formed from a hydrazone Schiff base ligand. Structural analysis using multiple spectroscopic and analytical methods confirmed an octahedral geometry, with metal ions coordinated through the azomethine nitrogen and hydroxyl oxygen atoms. DNA-binding behaviour was examined by UV–Vis absorption spectroscopy, viscosity studies, and thermal denaturation experiments, indicating a classical intercalative mode of binding, with binding constants reaching  $4.43 \times 10^6$  M<sup>-1</sup>. Agarose gel electrophoresis showed that these complexes efficiently promote oxidative cleavage of plasmid DNA, an effect associated with reactive oxygen species generated by the redox-active metal centres. Molecular docking studies revealed strong interactions of the complexes, especially those of Co (II) and Ni (II), with DNA binding sites. Furthermore, DFT calculations shows the electronic structures and frontier molecular orbitals of the complexes, which correlate well with their observed biological activity. Collectively, these findings indicate that the synthesized metal complexes are promising DNA-targeted therapeutic candidates with substantial potential for biological applications.

**Keywords:** Metal Complex; DNA Binding; Schiff Base; DFT; Molecular Docking.

**How to Cite:** Ereshanaik; M. C. Prabhakara; Nagendra Naik K.; Raghavendra S. M.; Surendranai Y. (2026) Synthesis, Characterization, Computational, DNA Binding and Cleavage Studies of Cu (II), Co (II), and Ni (II) Metal Complexes Derived N'-(E)-(3-hydroxynaphthalen-2-yl) methylidene] pyridine-4-carbohydrazide. *International Journal of Innovative Science and Research Technology*, 11(1), 3529-3546. <https://doi.org/10.38124/ijisrt/26jan1113>

## I. INTRODUCTION

In recent decades, the literature survey has presented that there has been many natural and synthetic ligands bearing N and O as donor atoms. These ligands were used to synthesize the metal complexes and are of great interest because of their ease of preparation, availability of their precursors such as primary amines, aldehydes, ketones and therapeutic & pharmacological usefulness in medicinal field [1-2]. They are also called imines or azomethines. These

compounds are classical ligands when substituted primary aromatic amines are used for condensation reaction with aromatic carbonyl compounds especially when aromatic precursors with hydroxyl, amine and thiol groups [3-4] present at ortho position which in turn make them polydentate ligands for instance, salen (tetridentate ligands), bistrans(comfortable cages for anion),rings and macro cycles (tetraaminebenzaldehyde), scorpeonates for transition metal chelates [5-6].

Schiff base hydra-zones are compounds containing biologically active (-CO-NH-N=CH-) pharmacophore and play significant roles in medicinal and pharmaceutical chemistry with many biological applications that comprise anti-tumour, anti-bacterial, anti-fungal, antioxidant and antimicrobial activity [7]. Schiff base ligands are well known for building wide variety of metal complexes extensively as metal ions in complexes which are stabilized in various oxidation states. Chemistry of derivatives of hydrazone Schiff base ligands with transition metal ions has gained much attention over the decades and enhancing the working capacity of metal ions in huge number of useful applications in biological, clinical, industrial, analytical along with their important roles in organic synthesis and catalysis [8].

Currently, Schiff base ligands obtained from pyridine-based aldehydes and hydrazides containing amine groups, along with their applications, have attracted considerable attention across many areas of chemistry and biological sciences, particularly in studies of DNA interactions such as binding and cleavage [9–10]. Metal complexes formed from polydentate Schiff base ligands are regarded as highly stable compounds because of the chelate effect. It has also been noted that there is significant interest in their applications when one or both of the amines and carbonyl components are heterocyclic aromatic systems, which has greatly advanced the development of coordination chemistry from both fundamental and applied perspectives.

DNA is a key biological target in the design of antibacterial, antifungal, antimalarial, antiviral, anticancer, and various other antimicrobial agents [11–13]. Depending on their mechanisms of action, these molecules are classified as inhibitors of nucleotide synthesis (methotrexate), polymerase inhibitors (cytarabine), DNA-template cleaving agents (cisplatin), and topoisomerase inhibitors (doxorubicin). In this context, studies on the interactions between small molecules and DNA are typically conducted as an initial step in assessing their potential therapeutic uses, because metal ions can influence both the extent and direction of a ligand's medicinal activity by altering its redox potential [14]. Consequently, the structure

and stability of metal chelates are especially important for understanding how they interact with DNA [15]. In addition, DNA cleavage can also occur as a result of such complexes binding to DNA. Since DNA is a key target in photodynamic therapy, any structural changes induced in DNA through its interaction with small molecules, followed by irradiation—arising, for instance, from the unusual behavior of the imine (C=N) bond may provide valuable insights.

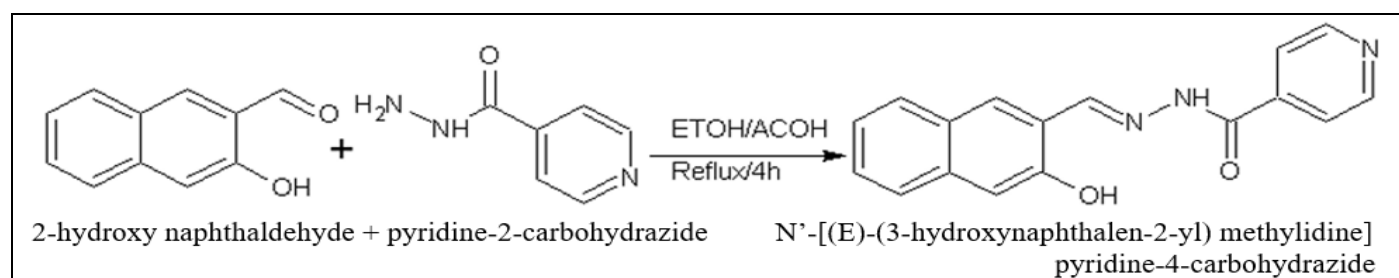
In view of the above facts, in this chapter, we have carried out synthesis of heterocyclic hydrazone Schiff base ligand which in turn utilized for synthesis of some transition metal complexes. Synthesized ligands and complexes have been characterized with various physio-chemical tools such as elemental analysis, FT-IR, <sup>1</sup>H-NMR, <sup>13</sup>C-NMR, U-V Spectrophotometer, mass spectrometer, PXRD method and Thermogravimetric analysis. Further, metal complexes have been screened for DNA binding and cleavage studies. Molecular modelling method has been exploited for theoretical comparison of DNA binding activity.

## II. EXPERIMENTAL

### ➤ Synthesis of Schiff Base Ligand

The Schiff base ligand was synthesized via a straightforward condensation protocol. An ethanolic solution of 2-hydroxynaphthaldehyde (0.02 mol) was combined with an ethanolic solution of pyridine-2-carbohydrazide (0.02 mol), and the resulting reaction mixture was refluxed for approximately 4 hours in the presence of a catalytic amount of glacial acetic acid. After cooling to ambient temperature, a colored solid precipitate formed, which was collected by filtration, washed repeatedly with dry diethyl ether, and subsequently recrystallized from ethanol. The synthesis of the Schiff base ligand, N'-(E)-(3-hydroxynaphthalen-2-yl) methylidene] pyridine-4-carbohydrazide, is depicted schematically below.

- *Scheme 1: Schematic Representation of Schiff Base Ligand*

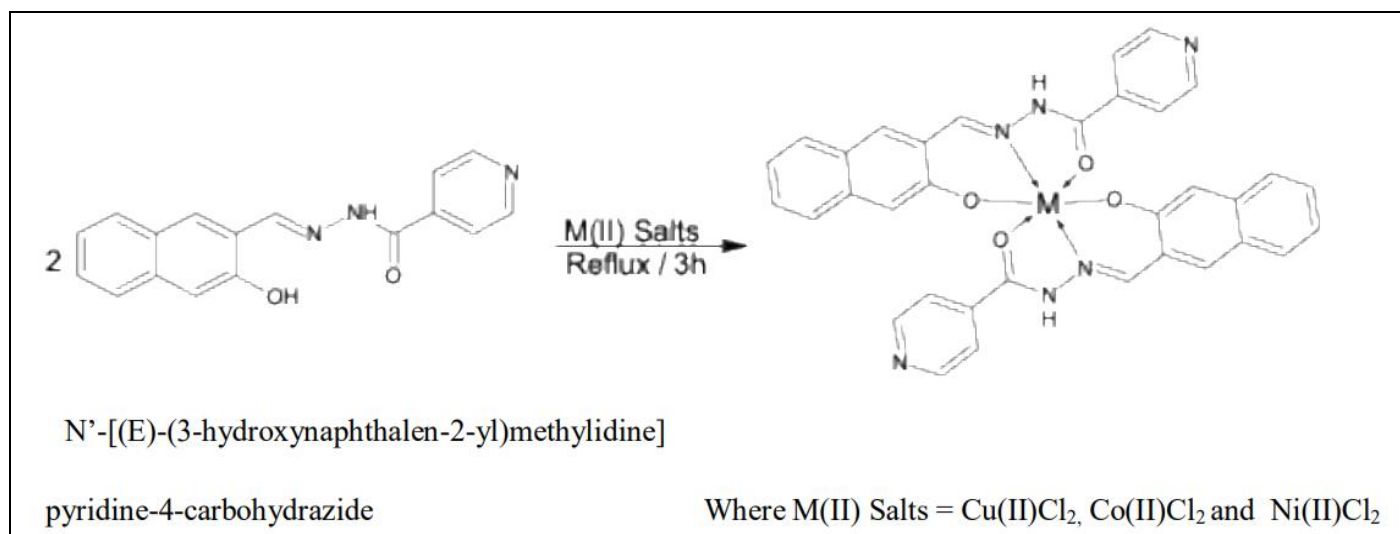


### ➤ Synthesis of Cu (II), Co (II), and Ni (II) Complexes

Metal(II) chlorides, including Cu(II), Co(II), and Ni(II) (1 mmol), and the synthesized Schiff base ligand (2 mmol) were dissolved in hot ethanol (EtOH) in a 1:2 metal-to-ligand molar ratio and refluxed in a water bath at 70–80 °C for 3 hours in the presence of triethylamine as a catalytic base. The reaction mixture was subsequently cooled to

ambient temperature, resulting in the formation of a solid precipitate. The isolated coordination complexes were collected by filtration and dried in a desiccator over anhydrous calcium chloride.

- *Scheme 2: Synthetic Route for the Synthesis of Metal Complexes.*



### III. RESULTS AND DISCUSSION

A hydrazone-based Schiff base ligand and its coordination complexes with Cu(II), Co(II), and Ni(II) were synthesized. The newly obtained species were rigorously characterized by a suite of physicochemical and spectroscopic techniques, including elemental (CHN) analysis, UV-Vis electronic absorption spectroscopy, FT-IR, <sup>1</sup>H and <sup>13</sup>C NMR spectroscopy, powder X-ray diffraction (PXRD), thermogravimetric analysis (TGA), and

mass spectrometry. In addition, the complexes were systematically investigated for their interactions with DNA, encompassing binding affinity and nuclease-mimetic cleavage activity. The electronic structures and related properties of the ligand and its coordination complexes were elucidated via Density Functional Theory (DFT) calculations. Molecular docking simulations were further employed to delineate and corroborate the DNA-binding modes of the transition-metal chelates.

Table 1 Physical and Investigative Data of Ligand and its Metal Complexes

Ligand / Complexes	Mol. Formula	Mol. Wt.	M P °C	Colour	Elemental Analysis (%) Calcd. (found)			
					C	H	N	M
Ligand	C <sub>17</sub> H <sub>13</sub> N <sub>3</sub> O <sub>2</sub>	291.30	211	pale Yellow	70.03 (69.92)	4.46 (4.14)	14.46 (13.92)	-- --
Cu(II) complex	C <sub>34</sub> H <sub>24</sub> N <sub>6</sub> O <sub>4</sub> Cu	644.13	> 300	Greenish brown	63.34 (62.88)	3.72 (3.16)	13.04 (12.62)	9.72 (9.42)
Co(II) complex	C <sub>34</sub> H <sub>24</sub> N <sub>6</sub> O <sub>4</sub> Co	639.67	> 300	Brown	63.86 (63.27)	3.98 (3.12)	13.35 (13.20)	9.16 (8.71)
Ni(II) complex	C <sub>34</sub> H <sub>24</sub> N <sub>6</sub> O <sub>4</sub> Ni	639.43	> 300	Reddish brown	63.88 (63.43)	3.88 (3.13)	13.36 (13.62)	9.16 (8.74)

#### ➤ FT-IR Spectral Analysis

The FT-IR spectrum of the free ligand was compared with those of its metal chelates to study the involvement of the ligand in the chelation process, as shown in Table 2. Figures 1–4 present the IR spectra of the ligand and its metal complexes.

The IR spectrum of the ligand exhibits a medium-intensity band at 3436 cm<sup>-1</sup>, attributable to the stretching vibration of a hydroxyl group [16], which is intramolecularly hydrogen-bonded to the adjacent nitrogen atom. The shift of this band in the spectra of all metal complexes indicates participation of the hydroxyl group in the chelation process. The band observed at 1620 cm<sup>-1</sup>, assignable to the azomethine (–HC=N–) moiety [17], is shifted to lower wavenumbers by 20–50 cm<sup>-1</sup> in the spectra of the synthesized metal complexes, suggesting the

involvement of the azomethine nitrogen in coordination and complex formation. Furthermore, the IR spectrum of the free ligand shows a strong absorption band at 1713 cm<sup>-1</sup> corresponding to the carbonyl (C=O) stretching vibration, which is shifted to lower frequencies by 40–60 cm<sup>-1</sup> upon complexation, confirming the participation of the carbonyl oxygen in chelation as evidenced in the IR spectra of the complexes [18]. New bands appearing at 463, 436, and 455 cm<sup>-1</sup> in the IR spectra of the Cu(II), Co(II), and Ni(II) complexes, respectively, are ascribed to  $\nu(\text{M}-\text{N})$  coordination modes. Similarly, bands at 599, 530, and 584 cm<sup>-1</sup> for Cu(II), Co(II), and Ni(II) complexes, respectively, are attributed to  $\nu(\text{M}-\text{O})$  vibrations. These spectroscopic features collectively indicate that the azomethine nitrogen and the oxygen donor atoms are actively involved in the metal–ligand coordination process. The spectral data for the ligand and its metal complexes are summarized in Table 2.

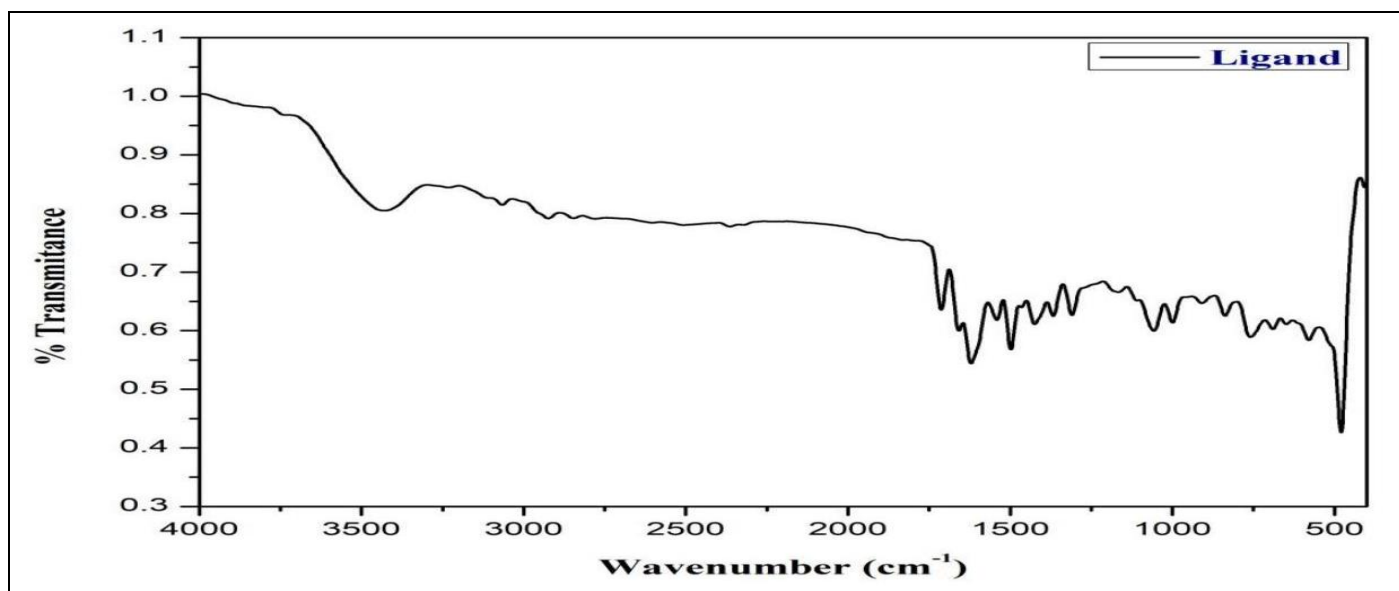


Fig 1 FT-IR Spectrum of the Hydrazone Schiff Base Ligand

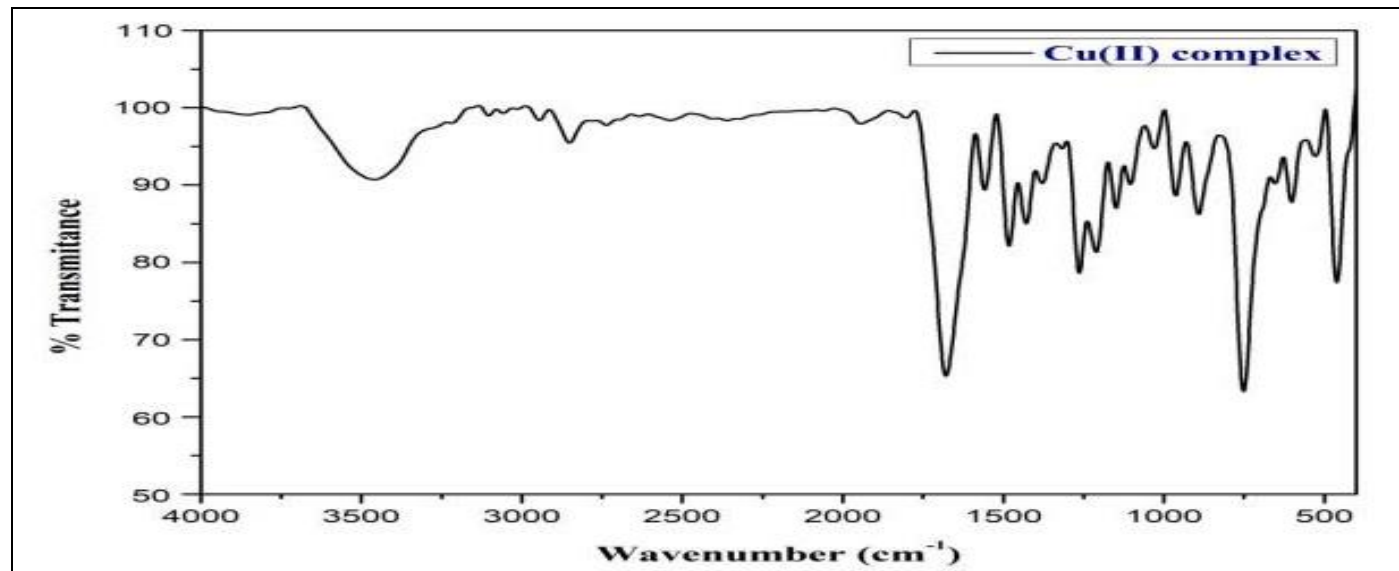


Fig 2 FT-IR Spectrum of Cu (II) Complex

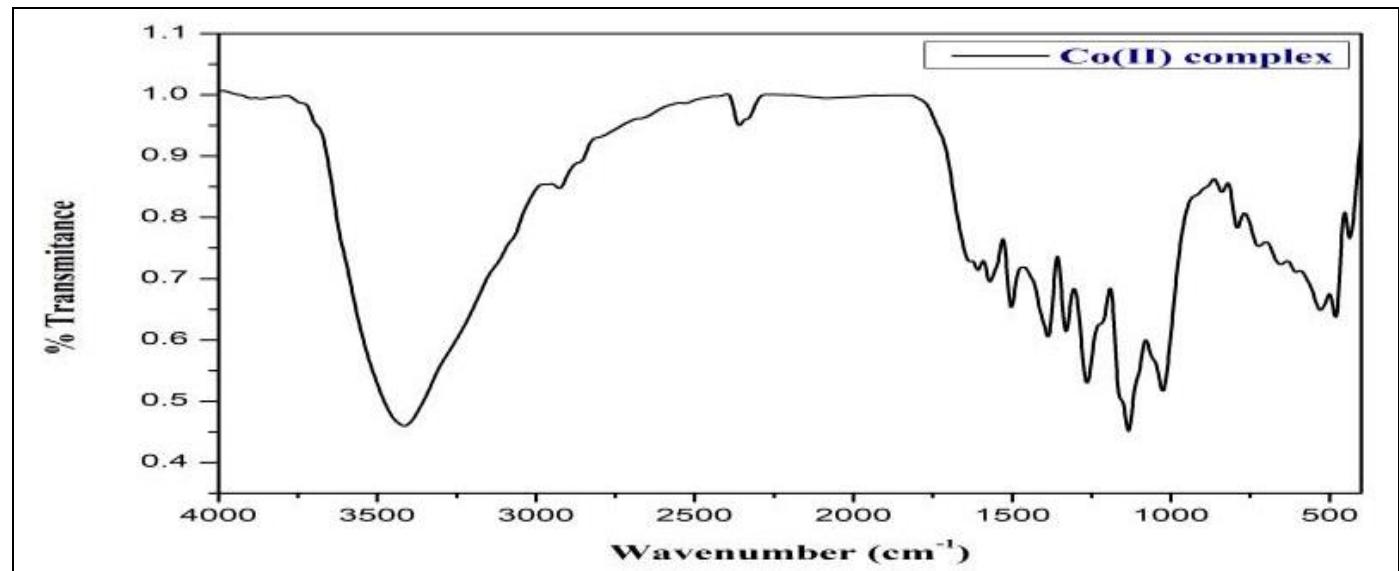


Fig 3 FT-IR Spectrum of Co (II) Complex

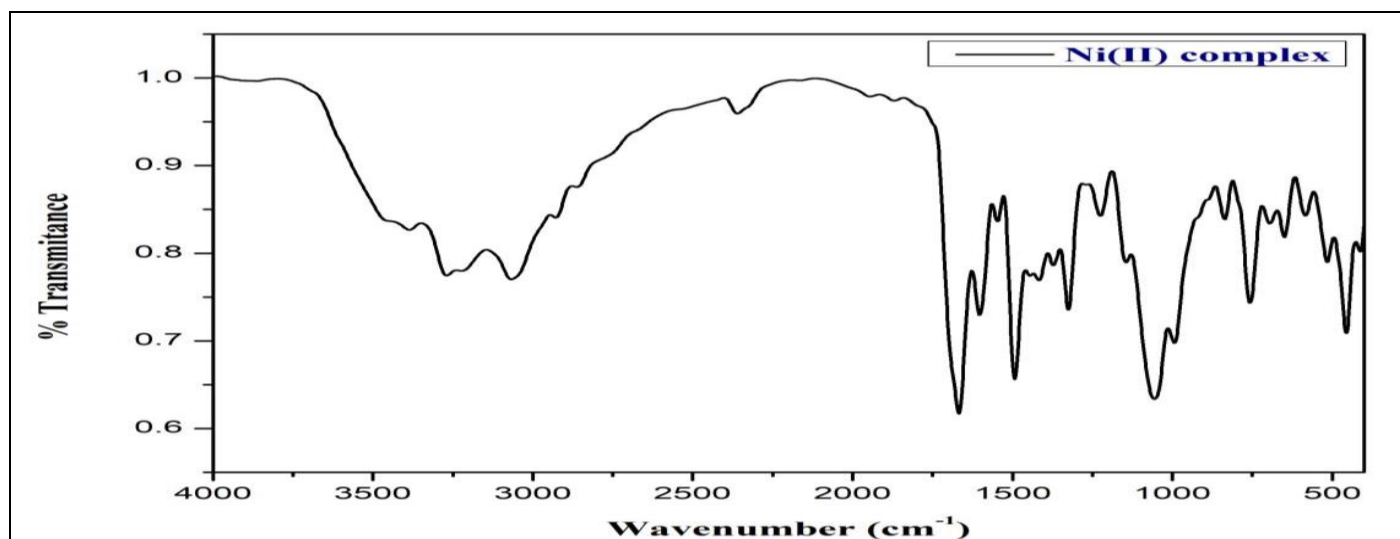


Fig 4 FT-IR Spectrum of Ni (II) Complex

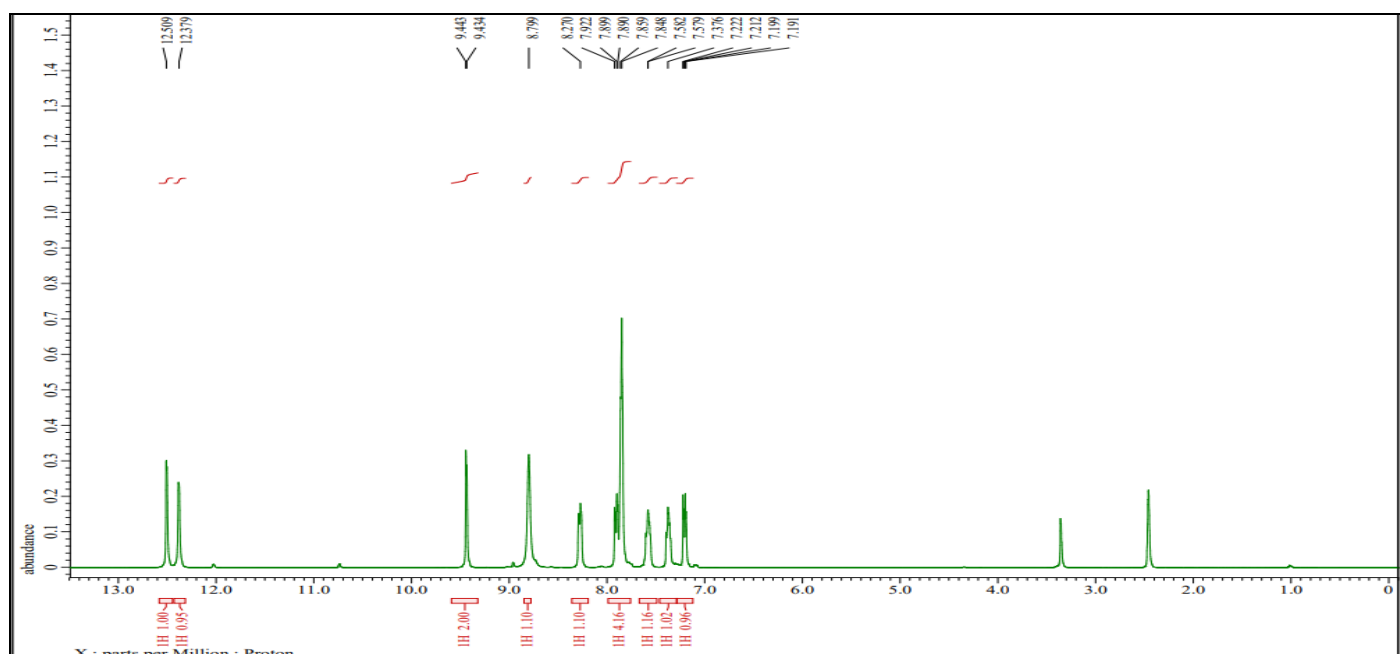
Table 2 Infrared Spectral Data of Compounds.

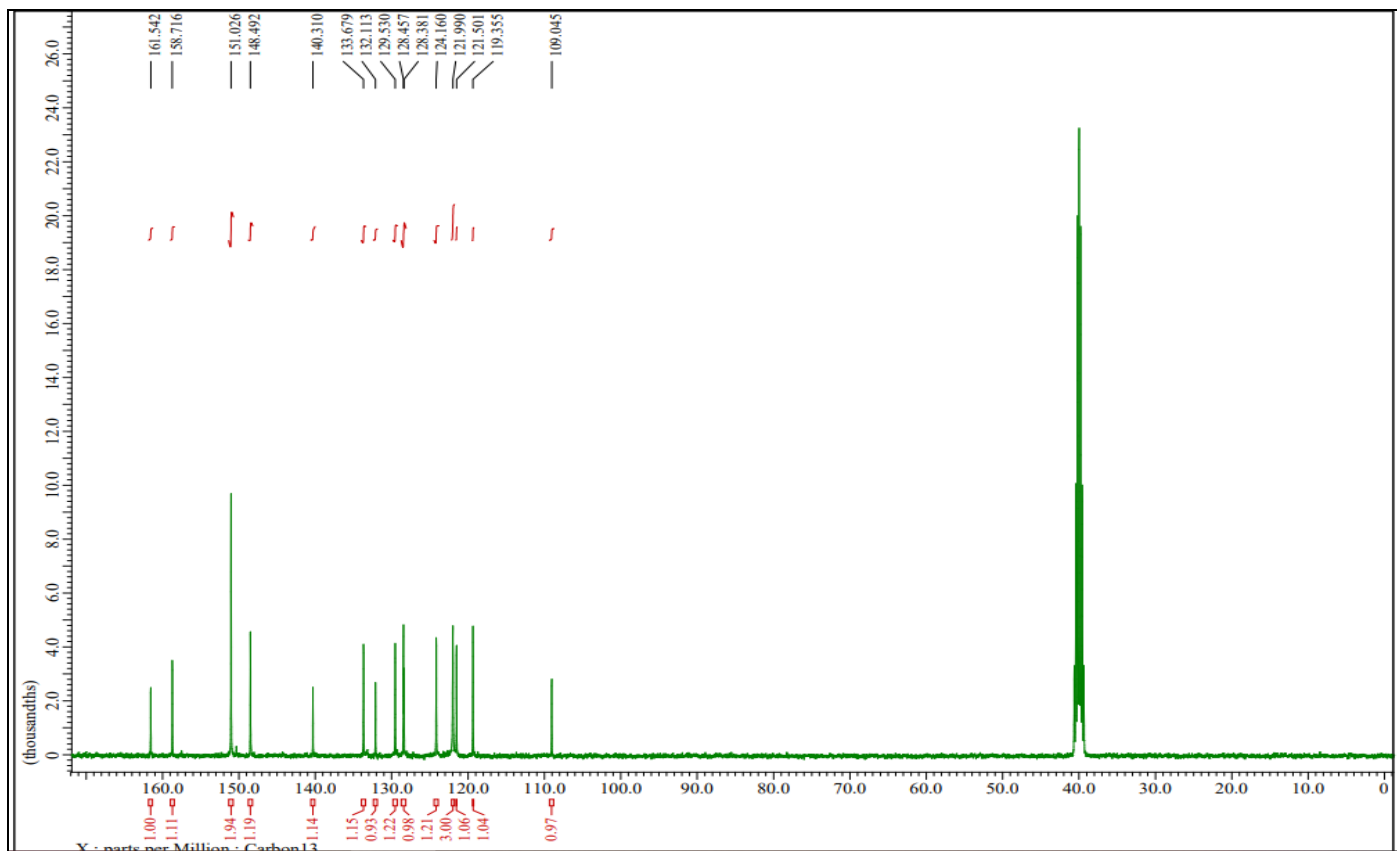
Ligand/ Complexes	$\nu$ (O-H) / H <sub>2</sub> O	$\nu$ (N-H)	$\nu$ (C=O)	$\nu$ (C=N)	$\nu$ (M-O)	$\nu$ (M-N)
Ligand	3436	3068	1713	1620	--	--
Cu (II) Complex	3460	3070	1678	1557	599	463
Co (II) Complex	3412	3060	1633	1571	530	436
Ni (II) Complex	3387	3062	1668	1602	584	455

#### ➤ <sup>1</sup>H & <sup>13</sup>C-NMR Analysis

The <sup>1</sup>H NMR spectrum of the ligand (Figures 5) exhibited resonances in the range 7.19–8.79 ppm, attributable to all non-equivalent aromatic protons [19]. Two downfield signals at 9.44 and 9.43 ppm are in good agreement with those expected for the azomethine (–CH=N–) proton of the Schiff base and the aromatic –CH=N moiety, respectively. Resonances at 12.50 and 12.37 ppm were assigned to the phenolic –OH and –NH protons, respectively, in the ligand spectrum [20–21].

The <sup>13</sup>C NMR spectrum of the synthesized ligand (Figures 6) displayed signals in the region 109.04–148.48 ppm, corresponding to the non-equivalent aromatic carbon atoms. A weak resonance at 151.02 ppm is consistent with the azomethine (–CH=N–) carbon of the Schiff base ligand. The carbon bonded to the hydroxyl group appeared at 158.71 ppm, while the carbonyl (C=O) carbon resonated at 161.54 ppm, in close agreement with previously reported hydrazone Schiff base systems. Collectively, the <sup>1</sup>H and <sup>13</sup>C NMR data corroborate the proposed structure of the synthesized hydrazone Schiff base ligand.

Fig 5 <sup>1</sup>H NMR Spectrum of the Hydrazone Schiff Base Ligand.

Fig 6  $^{13}\text{C}$  NMR Spectrum of the Hydrazone Schiff Base Ligand.

➤ *Mass Spectral Studies of Ligand and its Metal Complexes.*

Mass spectra of the ligand and the metal complexes were shown in Figures 7-10. The mass spectrum of the ligand has shown an  $m/z$  value of 291.3040 and was expected for the Schiff base ligand. The mass spectra of

Co(II), Ni(II) and Cu(II) complexes have shown  $m/z$  values of 639.8255, 639.5352 and 644.1387 which were expected at 639.5253, 639.2855 and 644.1387 respectively. These data suggested that the complexes were formed in the 1:2 ratio of ligand to metal ions.

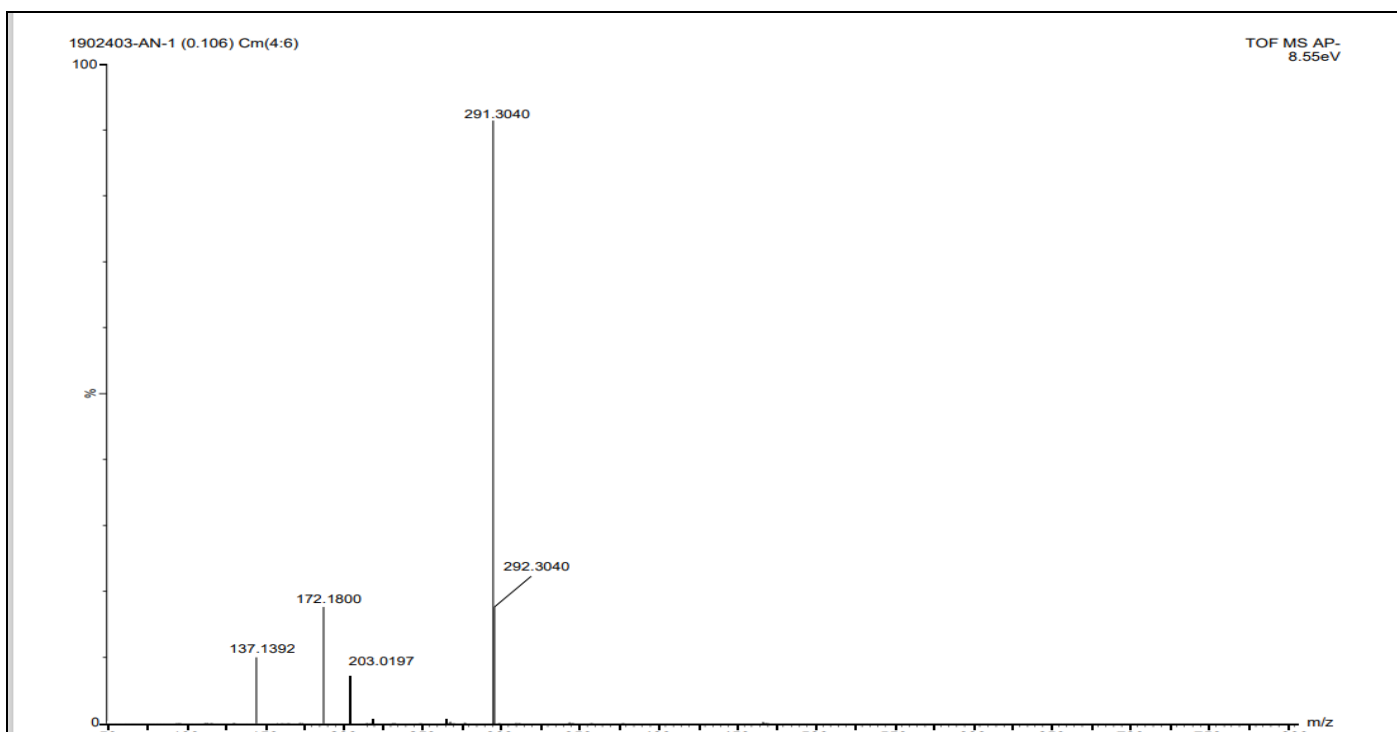


Fig 7 Mass Spectrum of the Hydrazone Schiff Base Ligand

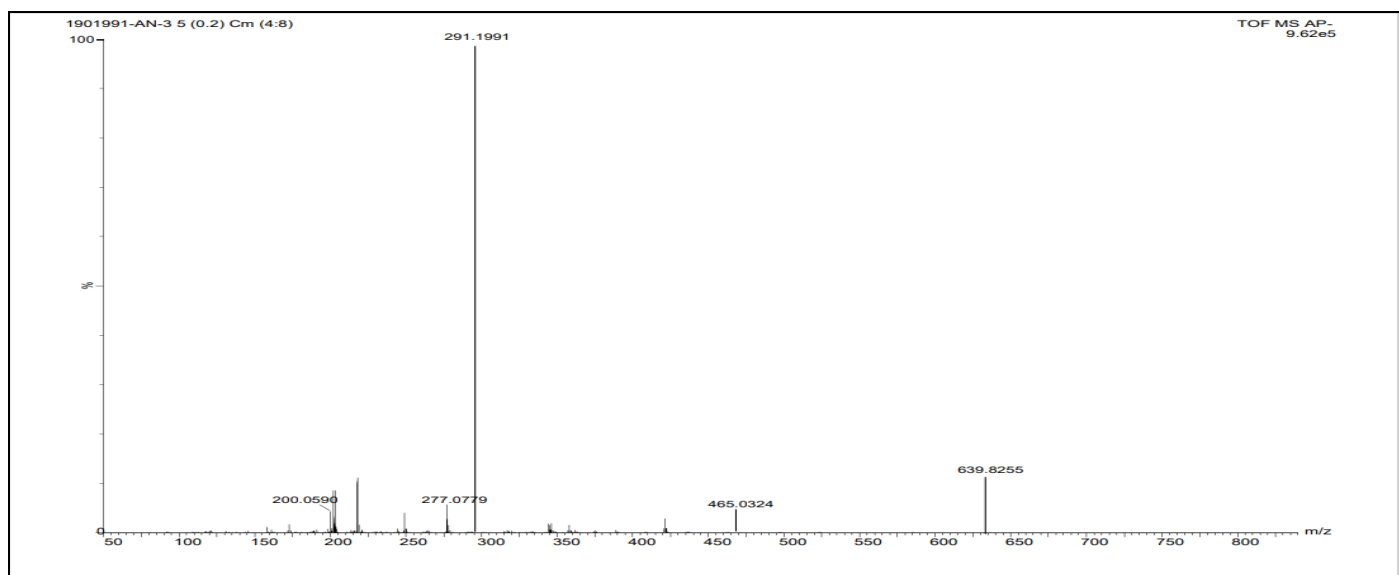


Fig 8 Mass Spectrum of the Co (II) Complex

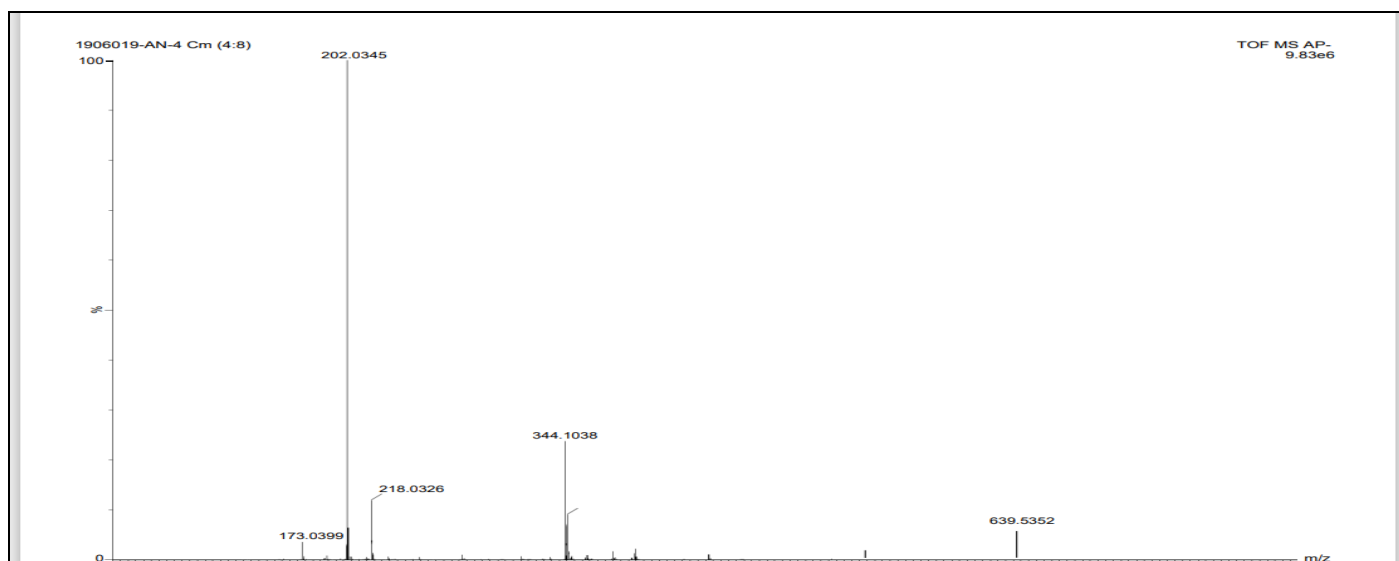


Fig 9 Mass Spectrum of the Ni (II) Complex

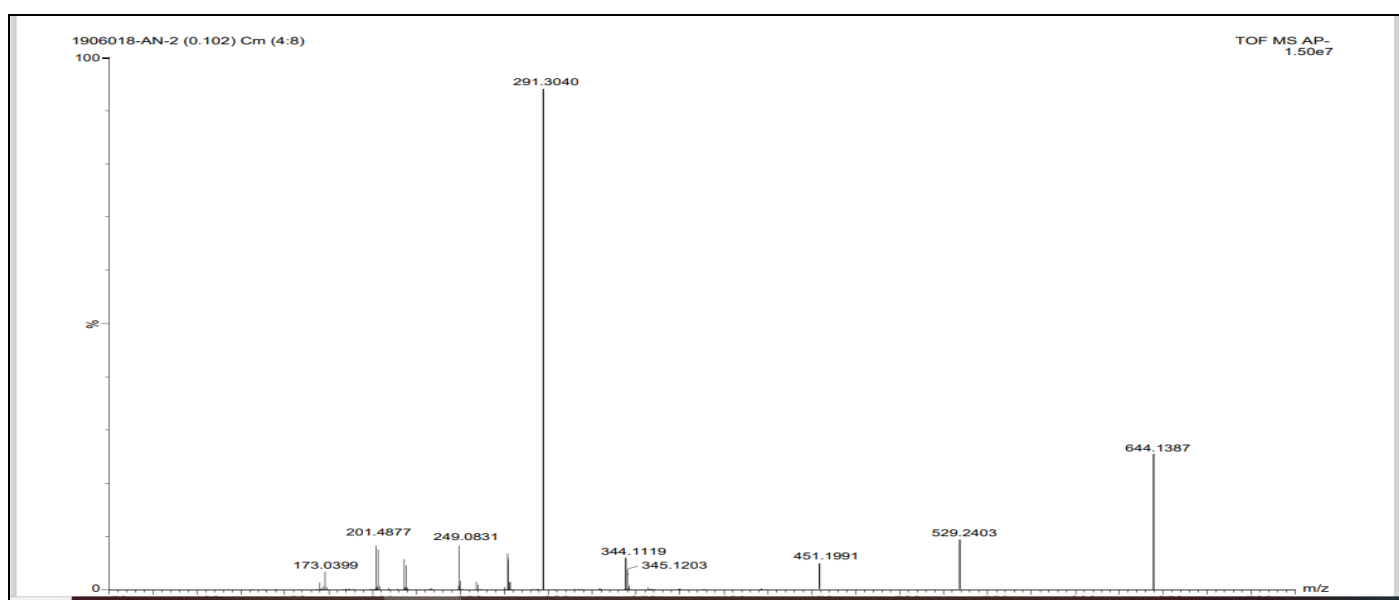


Fig 10 Mass Spectrum of the Cu (II) Complex

#### ➤ Ultraviolet-Visible Spectral Studies

The electronic absorption spectra of the compounds were recorded at ambient temperature in DMF as the solvent, as depicted in Figures 11. For the uncoordinated ligand, the absorption bands at  $38,883\text{ cm}^{-1}$  and  $32,739\text{ cm}^{-1}$  were assigned to  $\pi\rightarrow\pi^*$  and  $n\rightarrow\pi^*$  electronic transitions, respectively, while the band at  $22,441\text{ cm}^{-1}$  was ascribed to intra-ligand charge-transfer (ILCT) transitions of the Schiff base [22].

For the Cu(II) complex, the absorption band at  $20,573\text{ cm}^{-1}$ , attributable to the  $^2E_g\rightarrow^2T_{2g}$  transition arising from ligand-to-metal charge transfer (LMCT) [23], and its

spectral position are consistent with a distorted octahedral coordination environment, as further corroborated by the magnetic moment of 1.93 B.M. The Co(II) complex exhibits an absorption maximum at  $15,086\text{ cm}^{-1}$ , assignable to the  $^4T_{1g}\rightarrow^4T_{1g}$ ,  $^4T_{1g}\rightarrow^4T_{2g}$ , and  $^4T_{1g}\rightarrow^4A_{2g}$  transitions, which are characteristic of an octahedral field; the corresponding magnetic moment (4.24 B.M.) supports this assignment. Similarly, the Ni(II) complex displays an electronic absorption band at  $16,103\text{ cm}^{-1}$ , due to the d-d transitions  $^3A_2\rightarrow^3T_2$ ,  $^3A_2\rightarrow^3T_1$ , and  $^3A_2\rightarrow^3T_1$ , indicative of an octahedral geometry around the Ni(II) center, with a measured magnetic moment of 2.87 B.M.

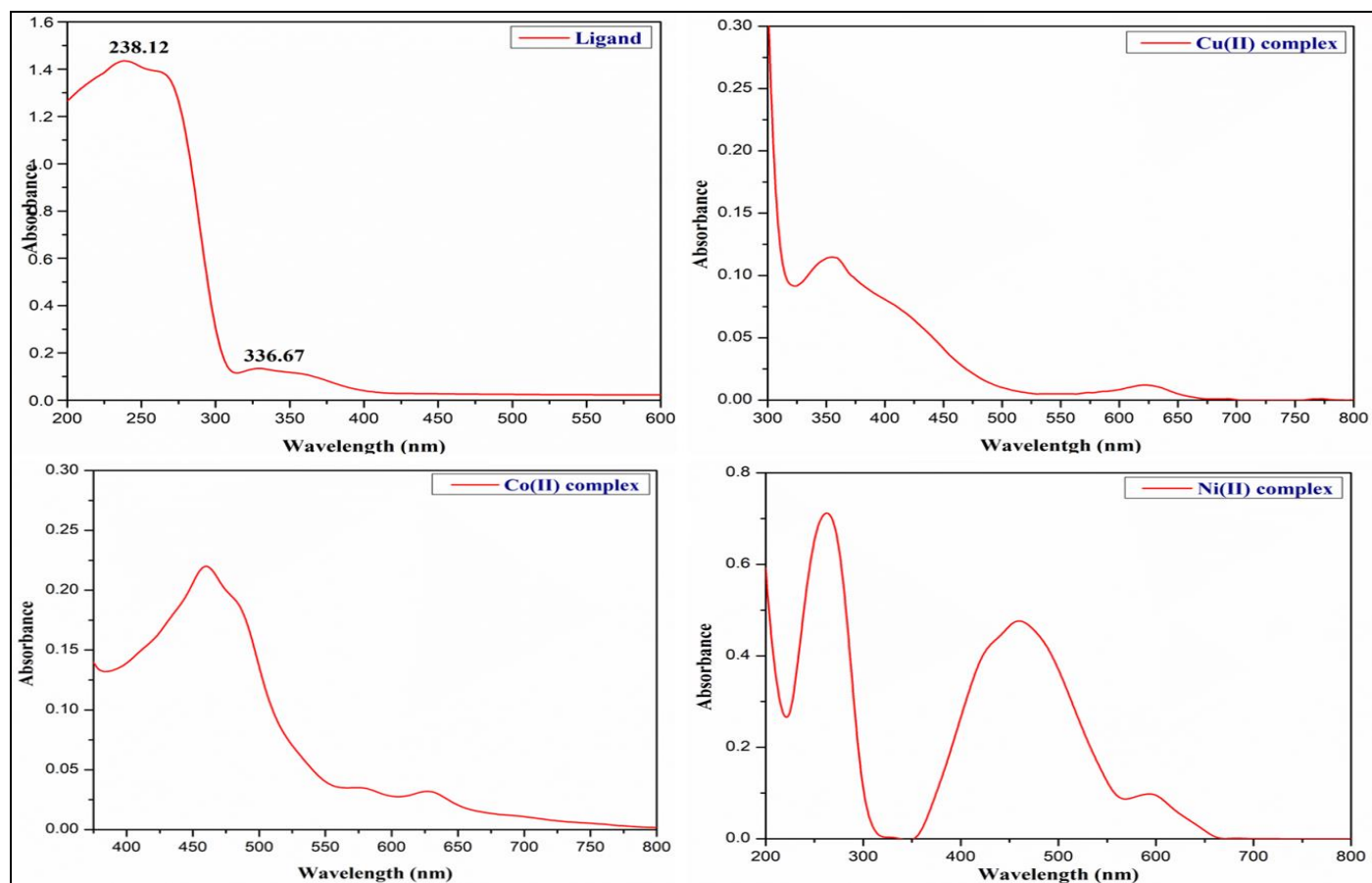


Fig 11 Electronic Spectra of Ligand and its Cu (II), Co (II), Ni (II) Complexes

#### ➤ PXRD Studies

Single crystals could not be obtained for all of the metal chelates, as these complexes are soluble in high-boiling polar aprotic solvents such as DMSO and DMF. Consequently, powder X-ray diffraction (PXRD) was employed to investigate the amorphous and partially crystalline solid forms of the metal complexes, providing insight into their solid-state structures. Diffractograms of the newly synthesized metal chelates were recorded over the  $2\theta$  range of  $5\text{--}80^\circ$  and are presented in Figures 12-14.

The PXRD patterns for the copper(II), cobalt(II), and nickel(II) complexes display 7, 8, and 8 distinct reflections, respectively, within the  $2\theta$  range of  $5\text{--}40^\circ$ . The squared  $h$ ,  $k$ ,  $l$  indices ( $h^2 + k^2 + l^2$ ) for these complexes were derived from the  $2\theta$  values, yielding 3, 7, 11, 12, 18, 25, and 31 for

Cu(II); 3, 5, 6, 7, 10, 17, and 21 for Co(II); and 3, 5, 10, 11, 16, 22, 28, and 30 for Ni(II). The  $h^2 + k^2 + l^2$  values, particularly the occurrence of the forbidden number 7, indicate that all of the metal complexes are most likely crystallizing in tetragonal and/or hexagonal crystal systems[24].

The corresponding lattice parameter  $a$  was calculated to be  $17.648\text{ \AA}$  for the copper chelate,  $8.924\text{ \AA}$  for the cobalt chelate, and  $17.272\text{ \AA}$  for the nickel chelate. The interplanar spacings ( $d$ ) and the relative intensities of the most prominent diffraction maxima serve as reliable structural descriptors. The partial crystallinity of the chelates is corroborated by the systematic attenuation of peak intensities from maximum to minimum across the diffraction patterns.

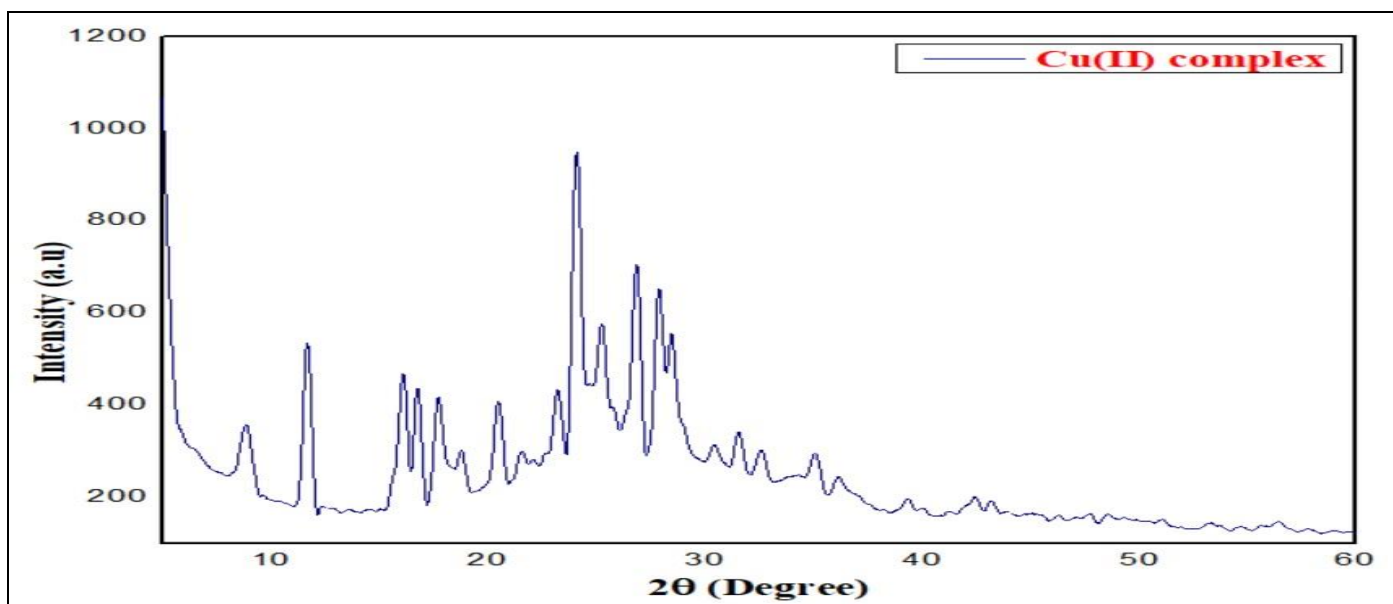


Fig 12 PXRD Spectrum of Cu (II) Complex

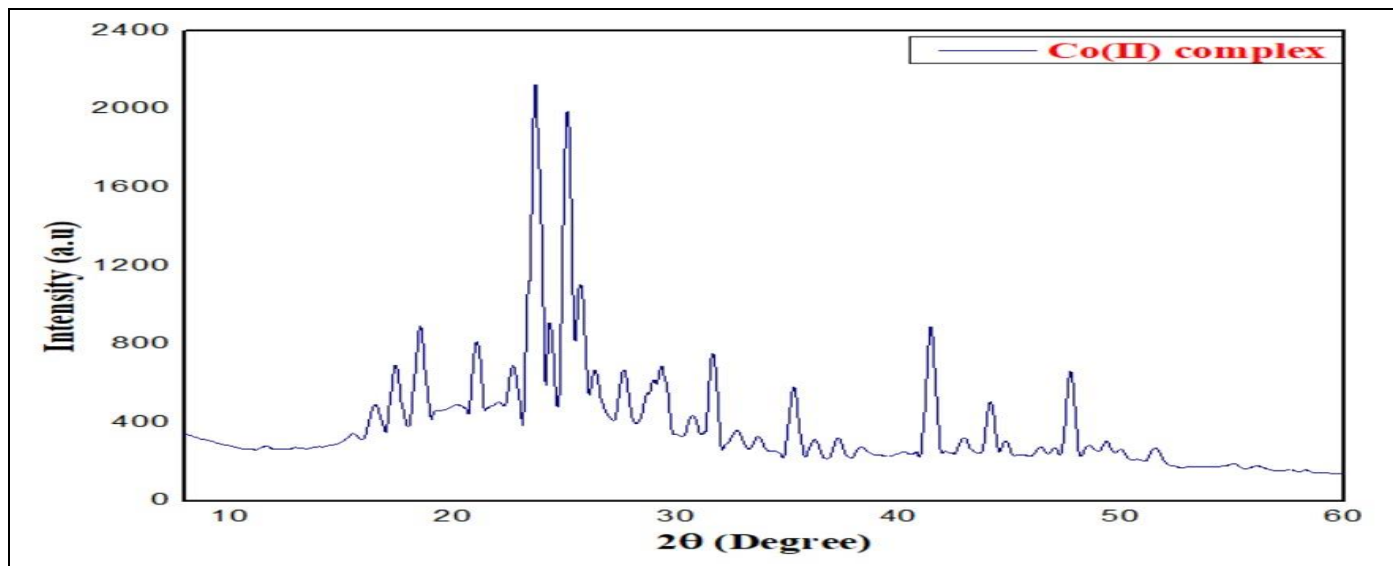


Fig13 PXRD Spectrum of Co (II)

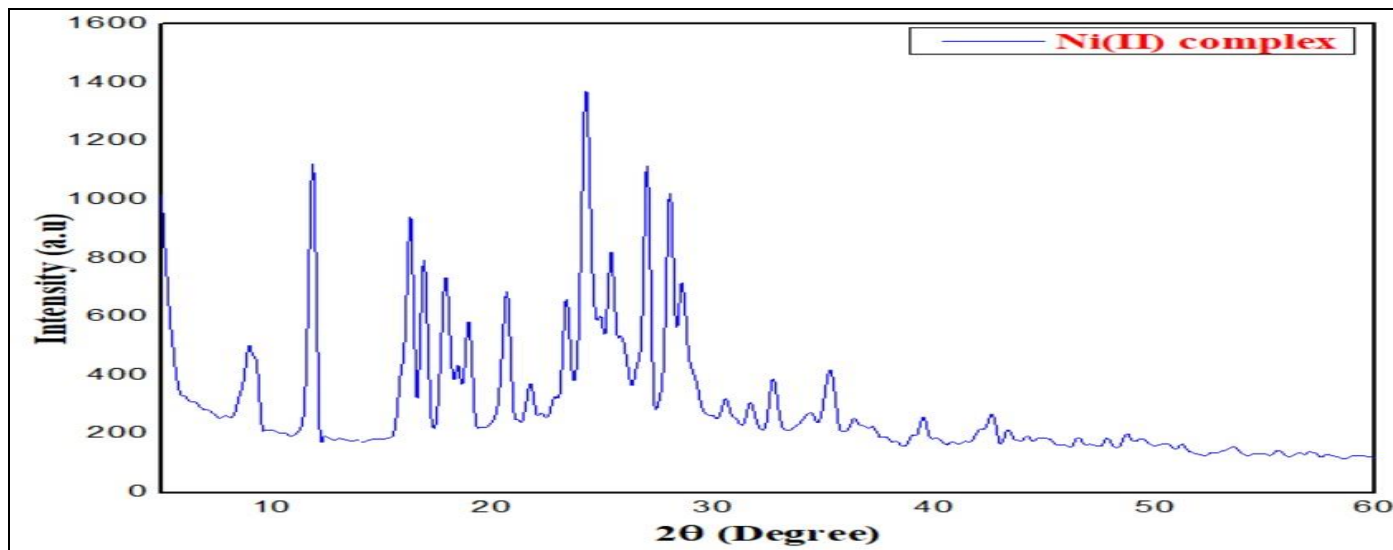


Fig 14 PXRD Spectrum of Ni (II) Complex

Table 3 [A]: PXRD Data for Cu (II) Complex

2θ	θ	sinθ	sin2θ	1000*sin2θ	$h^2 + K^2 + l^2$	m	hkl	d in Å*	a in Å*
8.67	4.33	0.075	0.005	5.7135	2.99975	3	111	10.22	17.71284
12.56	6.28	0.109	0.011	11.9655	6.58225	7	-	7.066	17.30964
16.34	8.17	0.142	0.020	20.1954	10.60314	11	113	5.439	18.04052
17.56	8.78	0.152	0.023	23.2992	12.23271	12	222	5.064	17.54282
21.06	10.53	0.182	0.033	33.3976	17.53466	18	114	4.229	17.94558
25.23	12.61	0.218	0.047	47.6980	25.0427	25	500	3.539	17.69699
28.23	14.11	0.243	0.059	59.4720	31.22439	31	-	3.169	17.64834

Table 4 [B]: PXRD Data for Co (II) Complex

2θ	θ	sinθ	sin2θ	1000*sin2θ	$h^2 + K^2 + l^2$	m	hkl	d in Å*	a in Å*
17.45	8.72	0.151	0.023	23.0104	3.000	3	111	5.095	8.8262
18.05	9.02	0.156	0.024	24.606	3.208	3	111	4.927	8.5351
21.45	10.72	0.186	0.034	34.631	4.515	5	120	4.153	9.2881
24.77	12.38	0.214	0.046	46.001	5.997	6	112	3.604	8.8281
28.67	14.33	0.247	0.061	61.301	7.292	7	-	3.122	8.8305
32.34	16.17	0.278	0.077	77.555	10.114	10	130	2.775	8.7775
42.06	21.03	0.358	0.128	128.77	16.789	17	140	2.154	8.8814
46.77	23.38	0.396	0.157	157.53	20.539	21	241	1.947	8.9248

Table 5 [C]: PXRD Data for Ni (II) Complex

2θ	θ	sinθ	sin2θ	1000*sin2θ	$h^2 + K^2 + l^2$	m	hkl	d in Å*	a in Å*
9.06	4.53	0.078	0.006	6.238	3.000	3	111	9.787	16.951
12.05	6.02	0.104	0.011	11.017	5.298	5	120	7.364	16.467
16.56	8.28	0.144	0.020	20.739	9.973	10	122	5.367	16.974
17.78	8.89	0.154	0.023	23.881	11.48	11	113	5.002	16.589
20.94	10.47	0.181	0.033	33.022	15.881	16	400	4.253	17.015
25.07	12.53	0.217	0.047	47.104	22.653	22	233	3.561	16.705
27.56	13.78	0.238	0.056	56.736	27.585	28	-	3.245	17.172
28.97	14.48	0.250	0.062	62.563	30.088	30	125	3.090	17.272

#### ➤ Thermogravimetric Analysis

An analytical method to study the nature of bonding of water, the thermal stability and composition of hydrazone based metal(II) complexes is known as Thermogravimetric analysis. A platinum pan under nitrogen gas was used to investigate the thermal nature of the complexes over a temperature range between 30 and 800 °C with temperature gradient of 10 °C/Min[25]. Thermogram of Cu(II) complex as depicted in the Figures 15 that complex was degraded in three steps. First degradation steps that ranges from 95-250 °C is attributable to the loss of water of hydration or coordinated to Cu(II) complex [26]. Second degradation step of the thermogram that ranges from 250-450 °C indicates partial decomposition of organic moiety of ligand, 450-525 °C is attributed to the complete degradation of organic ligand and the final step of degradation that

ranges from 525 °C which is indication of Copper oxide residue. Co(II) complex degraded in four steps as shown in the fig.5.15. The mass degradation at temperatures below 95-250 °C assignable to loss of water molecules of coordination or hydration. Two subsequent steps that ranges from 250- 350 °C and 350-450 °C indicate partial and complete degradation of organic part of the ligand followed by formation of Co(II)oxide residue at temperature range that starts from 550 °C. Similarly, mass degradation showed at 95-160 °C would be suggested for removal of hydrated or coordinated water molecule from Ni(II) complex. The second stage in the thermogram of Ni(II) complex shown in the Figures 15, that ranges from 340-425 °C attributable to complete removal of organic ligand and the third stage that starts from 425 °C is responsible for Ni(II)oxide residue.

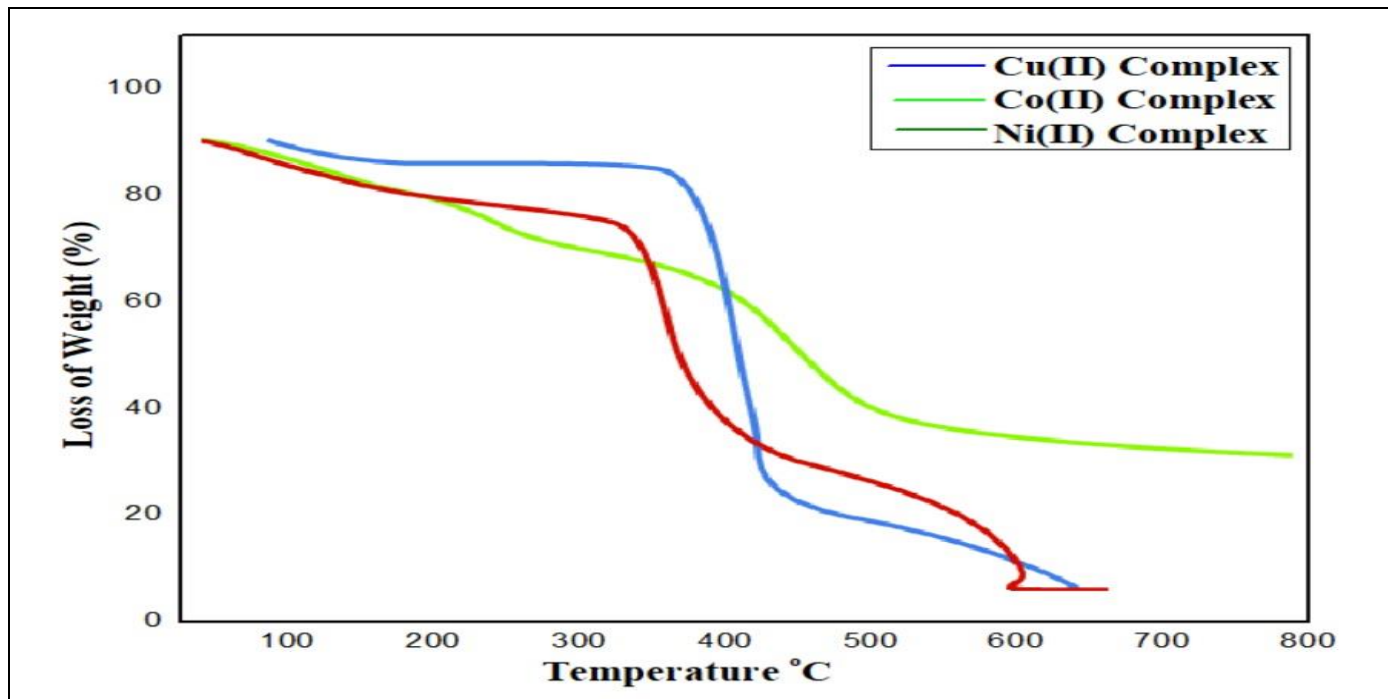


Fig 15 Thermogram of Co (II), Ni (II) and Cu (II) Complexes

#### IV. BIOLOGICAL STUDIES

##### ➤ DNA Binding Studies

###### • Absorbance Spectroscopy Studies

The absorption spectral investigation of CT-DNA interactions with the metal complexes was conducted in Tris-HCl buffer at pH 7.2, in both the presence and absence of DNA[27]. The experiments were performed at a fixed metal-complex concentration of 20  $\mu$ M[28], while varying

the CT-DNA concentration from 10 to 100  $\mu$ M, as illustrated in Figures 16-18. The resulting spectral data reveal that the observed hypochromism and hypsochromic (blue) shifts indicate that the metal complexes interact with calf thymus DNA via an intercalative binding mode[29–30]. The intrinsic binding constants ( $K_b$ ) of the complexes were determined to be  $1.83 \times 10^6 \text{ M}^{-1}$ ,  $4.43 \times 10^6 \text{ M}^{-1}$ , and  $2.73 \times 10^6 \text{ M}^{-1}$  for the Cu(II), Co(II), and Ni(II) complexes, respectively.

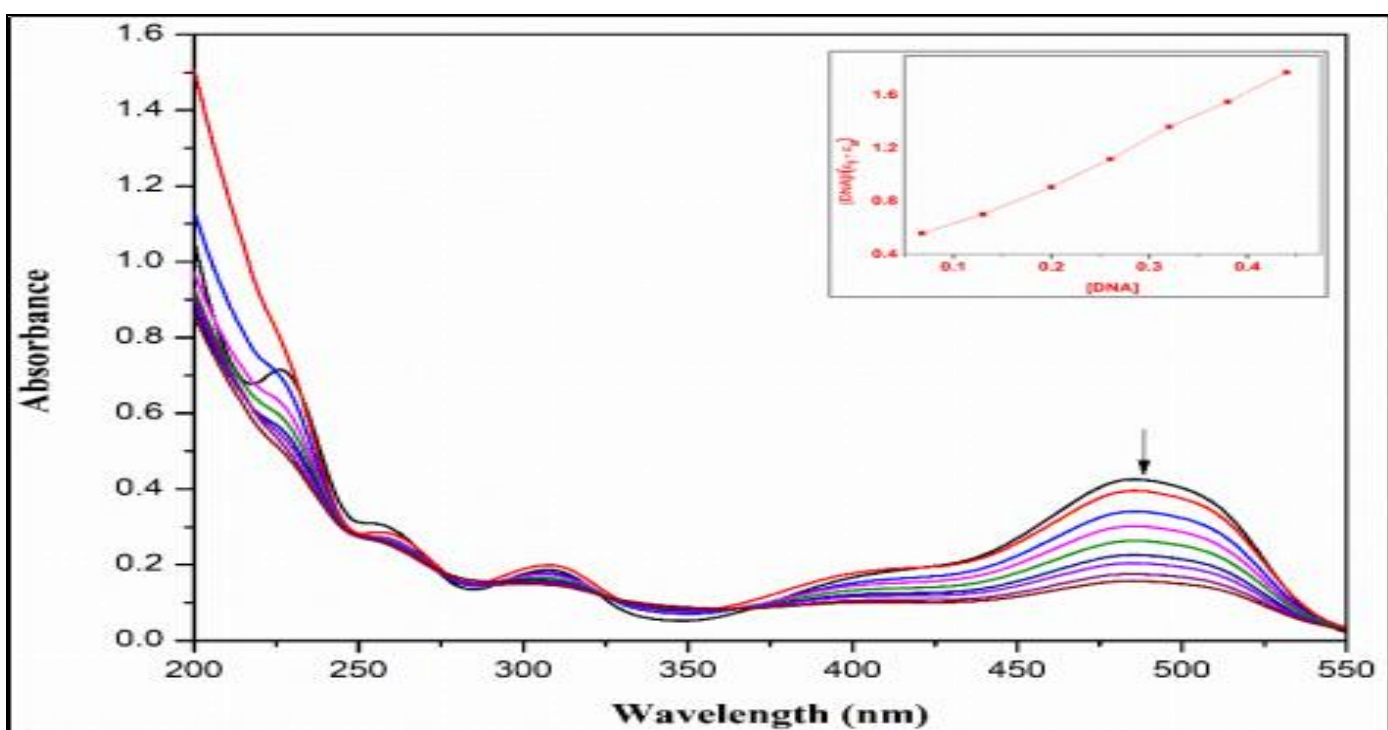


Fig 16 DNA Binding Study of the Cu(II) Complex by Absorption Spectroscopy Techniques.

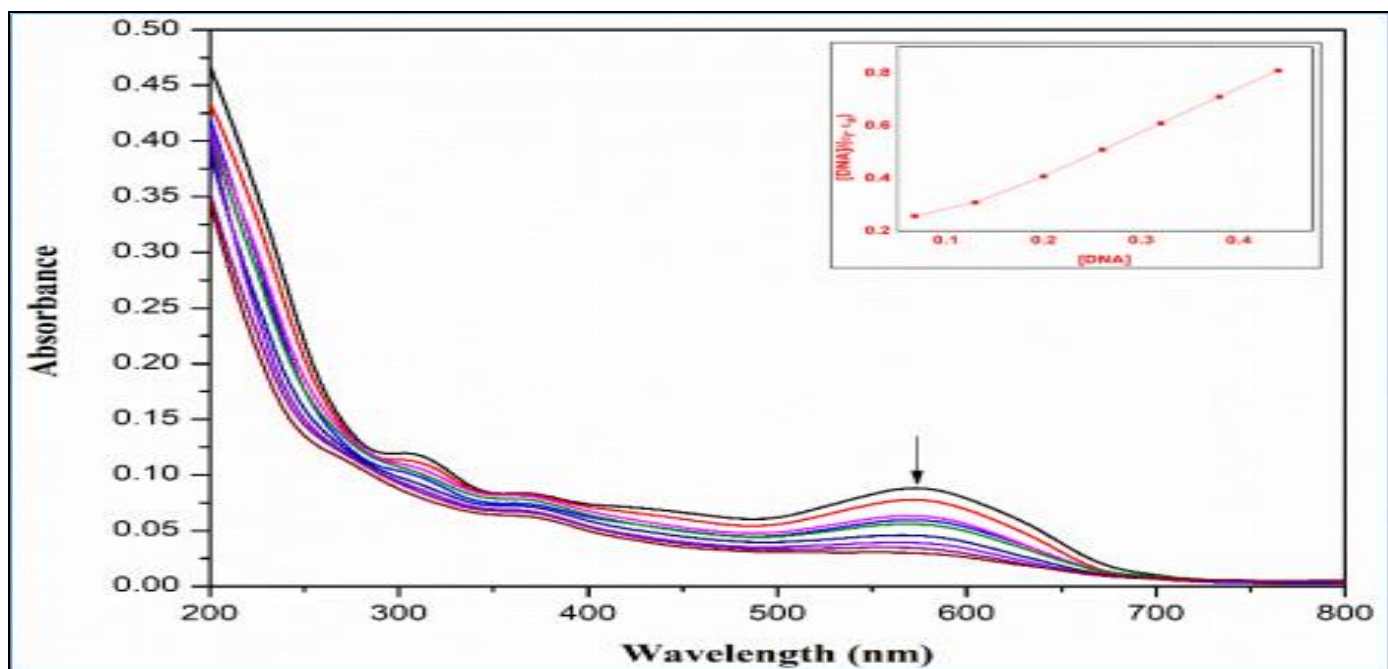


Fig 17 DNA Binding Study of the Co (II) Complex by Absorption Spectroscopy Techniques.

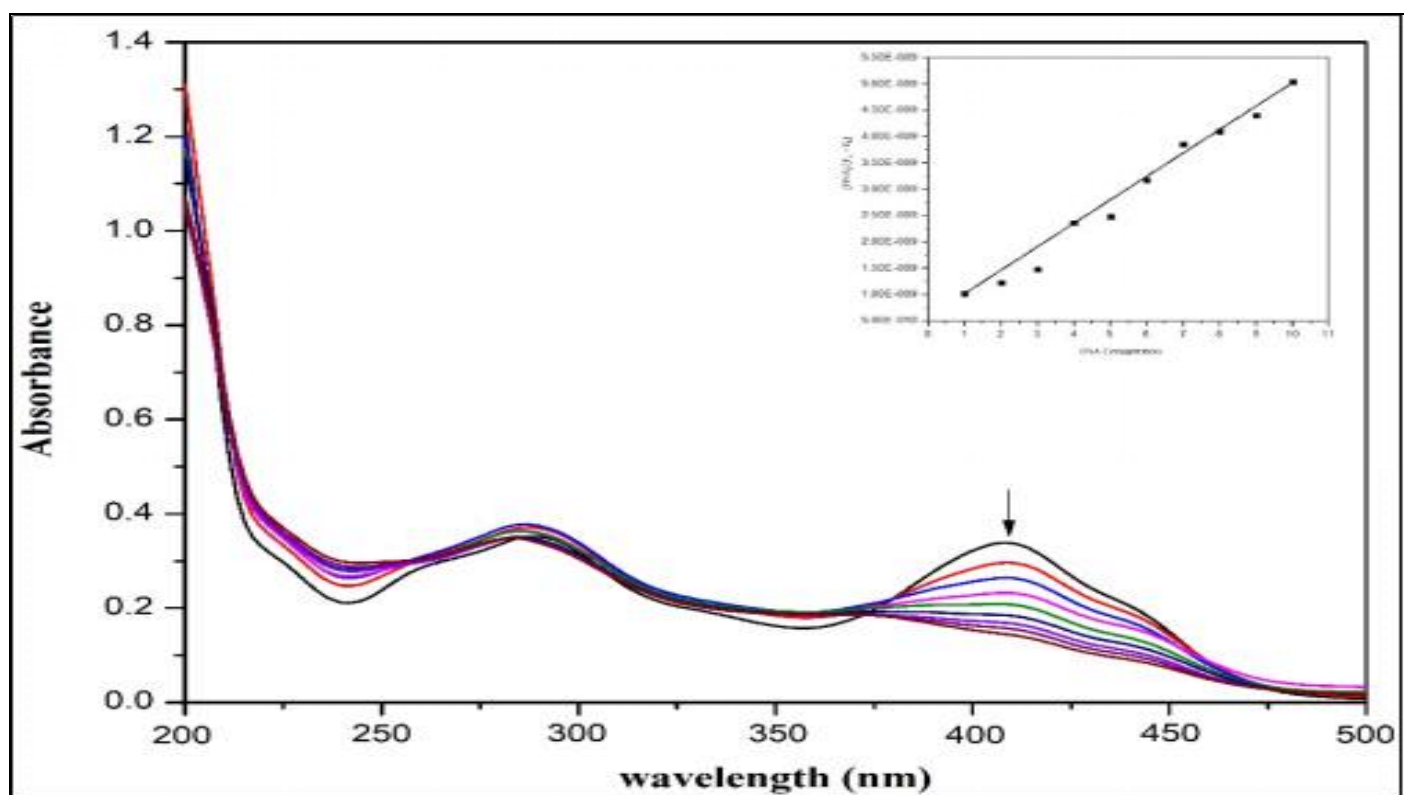
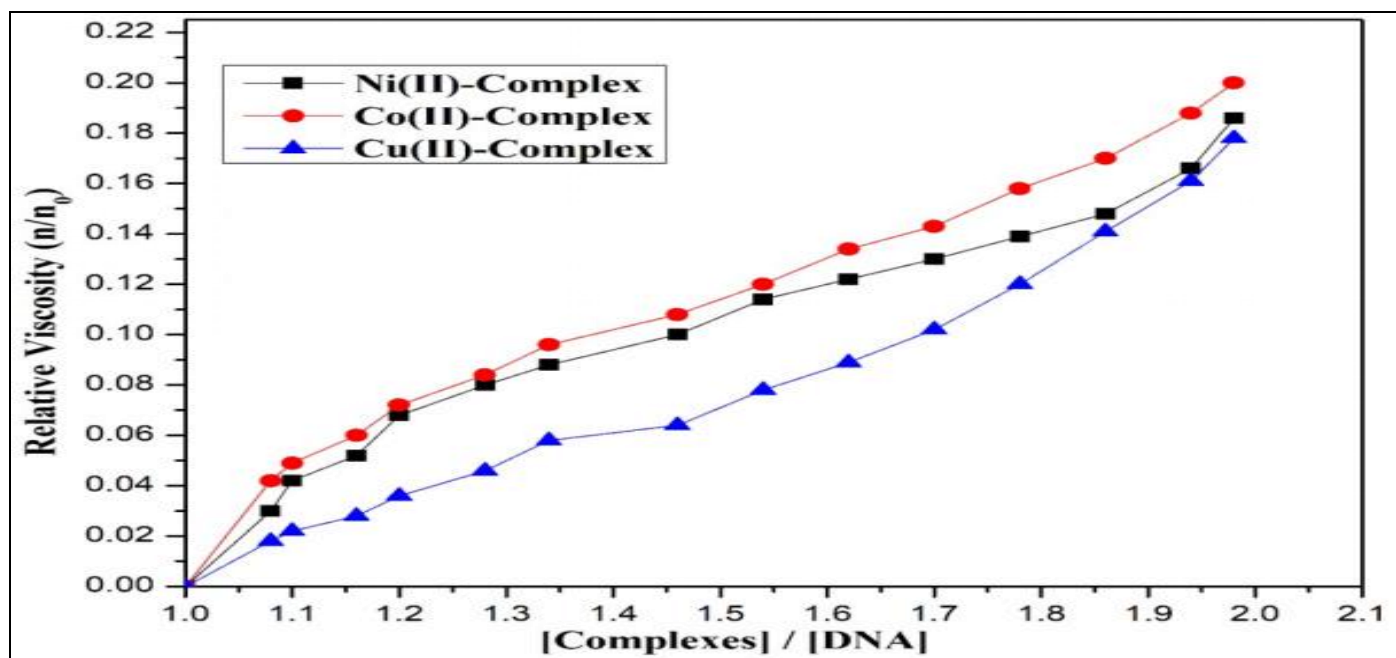


Fig 18 DNA Binding Study of the Ni (II) Complex by Absorption Spectroscopy Techniques.

#### ➤ Viscosity Measurements

This method is a broadly reliable tool for identifying how metal complexes bind to CT-DNA and is considered one of the most definitive techniques for characterizing DNA binding modes in solution when crystallographic data are unavailable. In classical intercalation, the DNA helix lengthens because the complexes insert between base pairs, which in turn increases the viscosity of the DNA solution. By contrast, partial intercalation can kink or bend the DNA

helix, reducing its effective length and thereby decreasing viscosity [31]. Non-intercalative modes, such as electrostatic or groove binding, generally produce only minor changes in viscosity. The influence of all the metal complexes on the viscosity of CT-DNA solution at  $28 \pm 1^\circ\text{C}$  is presented in Fig. 19. These results indicate that all the metal complexes interact with CT-DNA through an intercalative mode, and the viscosity measurements are in good agreement with the absorption study results.

Fig 19 Relative Viscosity of CT-DNA at 25 ( $\pm 0.1$ ) °C for Cu (II), Co (II), and Ni (II) Metal Complexes.

➤ *Thermal Denaturation Study*

The thermotropic behavior of DNA in the presence of coordination complexes provides critical insight into their conformational dynamics upon thermal perturbation and yields quantitative information regarding the interfacial binding strength of these complexes with calf thymus DNA (CT-DNA) [32]. In the present study, melting profile analyses of CT-DNA (100  $\mu$ M) revealed a melting temperature ( $T_m$ ) of  $64.3 \pm 1$  °C in the absence of any metal complex, as depicted in Fig. 20. Upon incremental addition

of the metal complexes (30  $\mu$ M), the  $T_m$  of CT-DNA increased markedly by approximately 4–8 °C, affording  $T_m$  values of  $68.6 \pm 1$  °C for the Cu(II) complex,  $69.4 \pm 1$  °C for the Co(II) complex, and  $68.3$  °C for the Ni(II) complex. These thermal denaturation data corroborate the electronic absorption titration results and collectively substantiate that all the investigated metal complexes interact with CT-DNA predominantly via a classical intercalative binding mode [33].

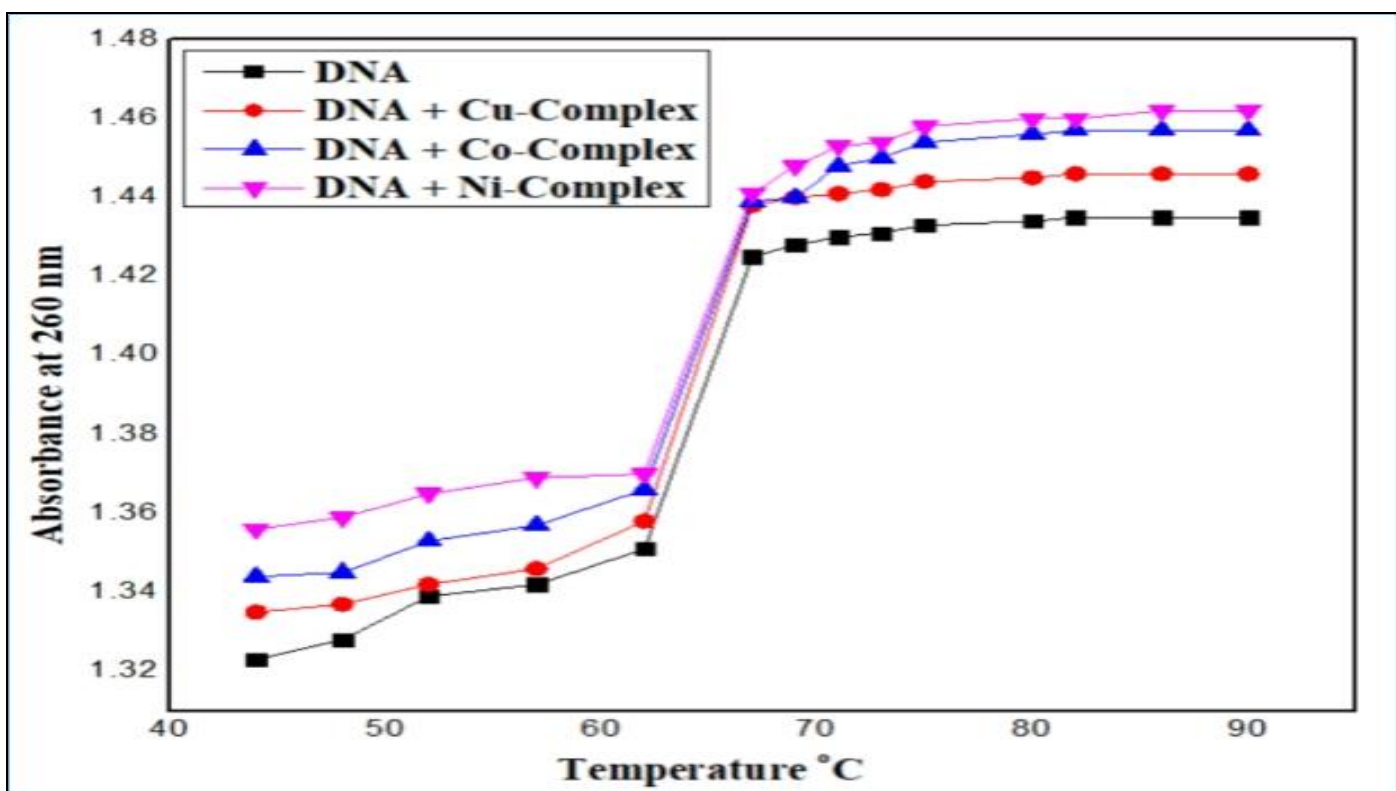


Fig 20 Thermal Denaturation Curves of CT-DNA in the Absence and Presence of Metal Complexes.

➤ *DNA Cleavage Studies Using the Gel Electrophoresis Method.*

The nuclease activity of the synthesized metal complexes toward pUC18 DNA was evaluated by agarose gel electrophoresis [34]. DNA strand scission was monitored by the conversion of the supercoiled (SC) plasmid form of pUC18 into its nicked circular (NC) topoisomer [35]. To assess the relative DNA-cleaving efficiency of the complexes, supercoiled pUC18 DNA was incubated with varying concentrations of the complexes for 1 h in 50 mM

Tris-HCl/50 mM NaCl buffer (pH 7.2). In the absence of metal complexes, no discernible DNA cleavage was detected, as evident in lane 1. In contrast, the complexes elicited pronounced and concentration-dependent cleavage of pUC18 DNA at 20, 40, and 60  $\mu$ M. The electrophoretic profiles demonstrated that, at these concentrations, pUC18 DNA cleavage was efficiently mediated by all metal complexes, as observed in lanes 3–11 and illustrated in Fig. 21.

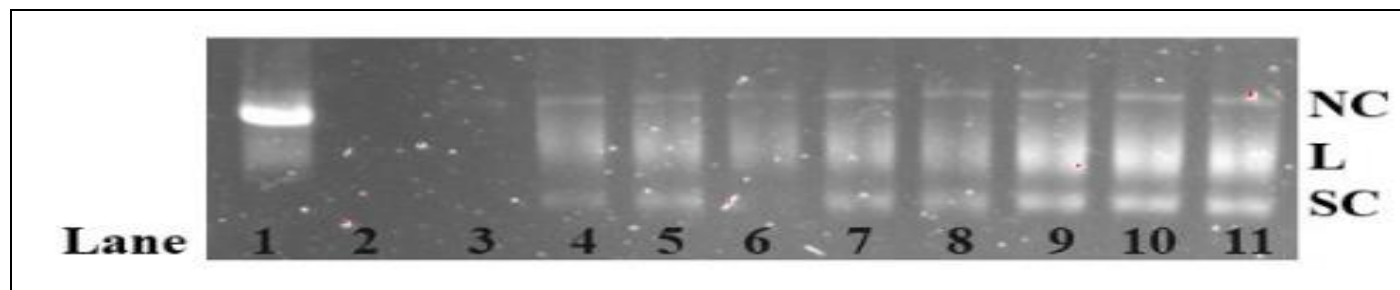


Fig 21 Cleavage of Supercoiled pUC18 DNA by Metal Complexes. Lane 1: DNA Alone; Lane 2: DNA +  $\text{H}_2\text{O}_2$ ; Lane 3: DNA + 20  $\mu\text{M}$  Copper Complex; Lane 4: DNA + 40  $\mu\text{M}$  Copper Complex; Lane 5: DNA + 60  $\mu\text{M}$  Copper Complex; Lane 6: DNA + 20  $\mu\text{M}$  Cobalt Complex; Lane 7: DNA + 40  $\mu\text{M}$  Cobalt Complex; Lane 8: DNA + 60  $\mu\text{M}$  Cobalt Complex; Lane 9: DNA + 20  $\mu\text{M}$  Nickel Complex; Lane 10: DNA + 40  $\mu\text{M}$  Nickel Complex; Lane 11: DNA + 60  $\mu\text{M}$  Nickel Complex.

Moreover, DNA scission is promoted through the generation of reactive oxygen species (ROS), which are, in turn, catalytically produced by the metal complexes. Consequently, metal ions serve as critical molecular cofactors for the ligand, facilitating redox cycling that culminates in ROS production. In the presence of transition metal ions such as Cu(II), Co(II), and Ni(II), chelating agents elicit ROS formation via Fenton-like oxidative processes. The quasi-reversible M(II)/M(I) redox couple

activates  $\text{H}_2\text{O}_2$ , yielding highly reactive  $\cdot\text{OH}$  radicals that constitute key effectors in DNA strand cleavage [36].



Due to their high reactivity and small diffusion radius, hydroxyl radicals must be generated in close proximity to DNA to effectively induce DNA strand scission, as illustrated in Fig 22.

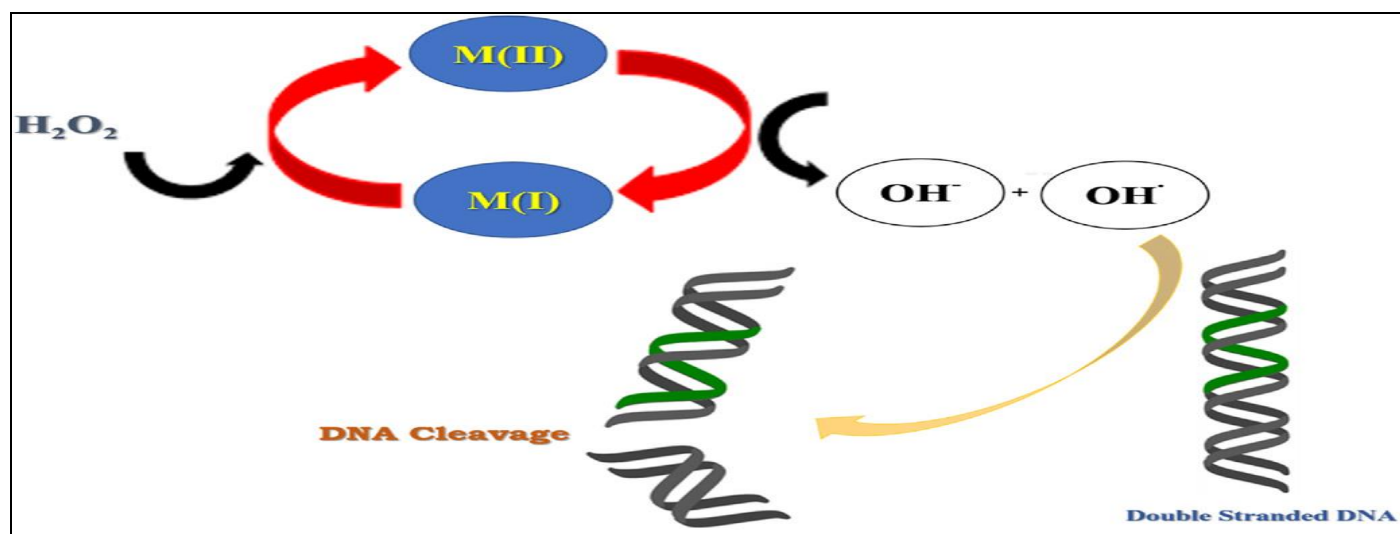


Fig 22 Mechanism of ROS Generation and DNA Cleavage.

## V. MOLECULAR DOCKING WITH DNA

The architectures of the Co, Cu, and Ni coordination complexes were subjected to molecular docking against the DNA-binding receptor (PDB ID: 1E3Y). The receptor-ligand interaction energies were computed via *in silico*

docking employing the HEX 8.2 engine, and the corresponding docking scores are compiled in Table 1. The DNA-binding docking outcomes demonstrate thermodynamically favorable interactions for the Co and Ni complexes, which display enhanced affinity toward the 1E3Y receptor relative to the Cu complex, with minimum

binding energies of  $-332.42$ ,  $-331.20$ , and  $-313.29$  kcal mol $^{-1}$ , respectively. Detailed docking analysis indicates that the dominant interaction forces between Co(II)/Ni(II) centers and the receptor's active-site residues comprise hydrogen-bond acceptor/donor contacts and metal-ligand coordination interactions. Furthermore, the Co(II) and Ni(II) complexes participate in electrostatic ( $\pi$ -anion) and hydrophobic ( $\pi$ - $\pi$  stacking,  $\pi$ -alkyl) noncovalent interactions with amino acid residues in the protein environment proximal to the ligand. The carbonyl oxygen atoms and the coordinated nitrogen atom(s) in the Co(II) and Ni(II) complexes are implicated in the formation of

stabilizing hydrogen bonds with ALA476, ASN477, GLY478, THR44, ALA45, ARG46, GLN47, ALA48, LEU49, ASN50, ASP51, ASP52, GLU53, PHE54, LYS55, ASP479, ALA480, TRP481, VAL482, PHE483, LYS484, GLY485, GLY486, GLN56, HIS84, ASP85, VAL86, THR87, ASP88, ALA89, ALA90, SER91, TYR92, ALA93, VAL94, LEU95, LYS96, VAL118, ALA119, PRO120, ARG121, PHE122, PHE123, GLY124, THR125, ILE126, ALA127, LYS128, TYR129, LEU130, LYS131. The optimal docked orientations of the Co and Ni complexes with the 1E3Y receptor are shown in Fig. 23.

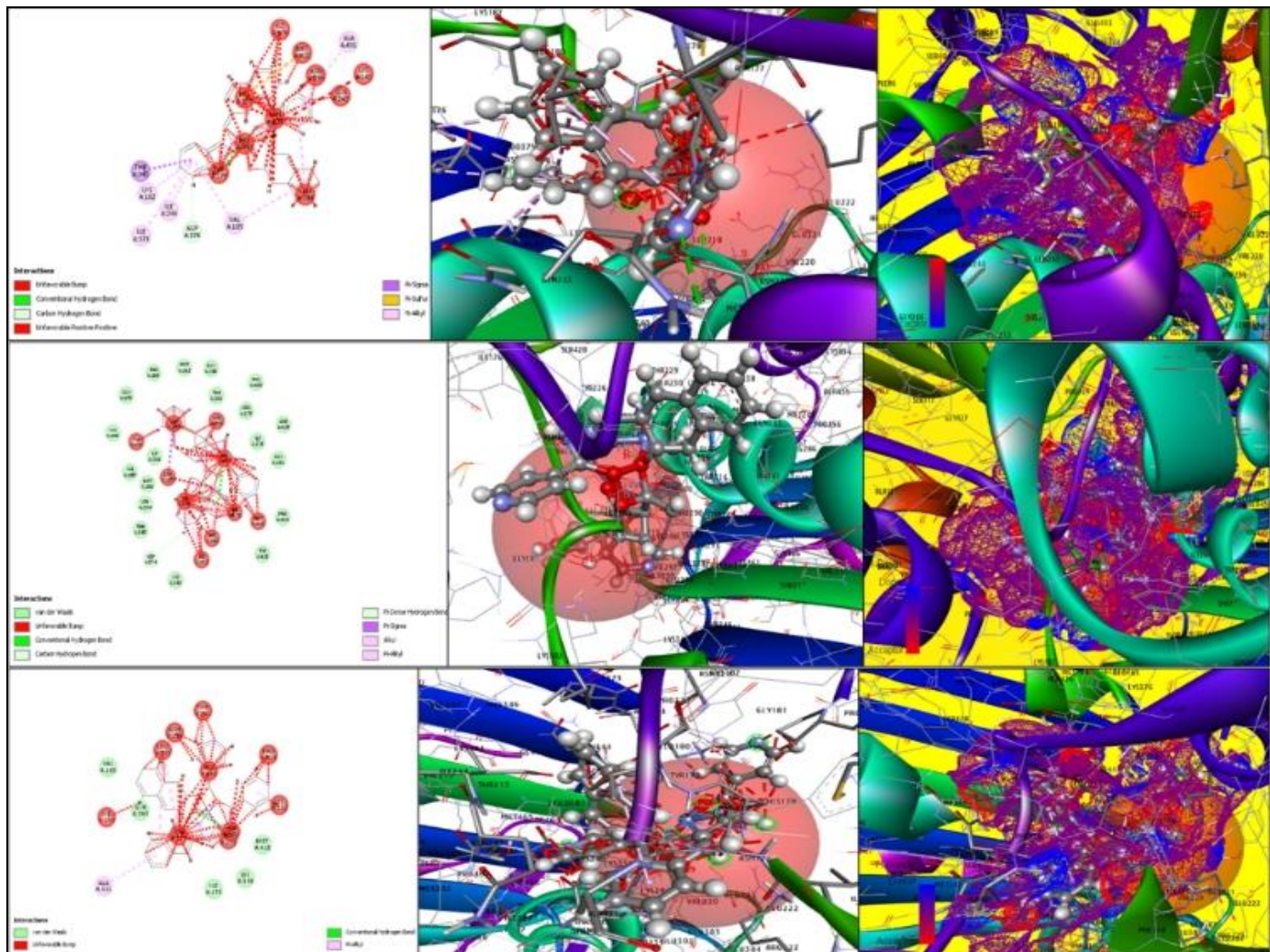


Fig 23 Different Modes of Binding Interaction of Cu (II) Complex with Receptor 1E3Y (a) 2D Interaction (b) 3D Interaction (c) Hydrogen Bonding Interaction.

## VI. DENSITY FUNCTIONAL THEORY

Density functional theory (DFT) constitutes a pivotal computational paradigm for elucidating diverse intra-molecular electronic interactions. The HOMO–LUMO electronic structures of the Schiff base ligand and its corresponding metal chelates were computed employing the RB3LYP exchange–correlation functional in conjunction with the 6-311G(++,g,d,p) basis set, and the fully optimized geometries of the free ligand and its complexes are illustrated in Fig. 24. The associated quantum-chemical

descriptors, including the frontier orbital energies (EHOMO and ELUMO) [37], are compiled in Table 6.

To interrogate the frontier orbital energy-level characteristics of the Schiff base ligand and its metal chelates, detailed analyses of the HOMO and LUMO were undertaken. Additionally, Frontier Molecular Orbital (FMO) analysis of the ligand and its complexes affords deeper insight into their intrinsic electronic structures and reactivity patterns. For the free Schiff base ligand, both HOMO and LUMO electron densities are predominantly delocalized

across the entire  $\pi$ -conjugated framework, with an associated HOMO–LUMO energy separation of 0.15128 eV. For the Cu(II), Co(II), and Ni(II) complexes, the computed band gaps are 0.14055 eV, 0.14755 eV, and 0.17071 eV, respectively, consistent with predominant  $\pi$ – $\pi^*$

intraligand charge-transfer transitions. The spatial distributions of the FMOs for the Schiff base ligand, its metal chelates, and the corresponding frontier orbital energy levels are presented in Fig. 24.

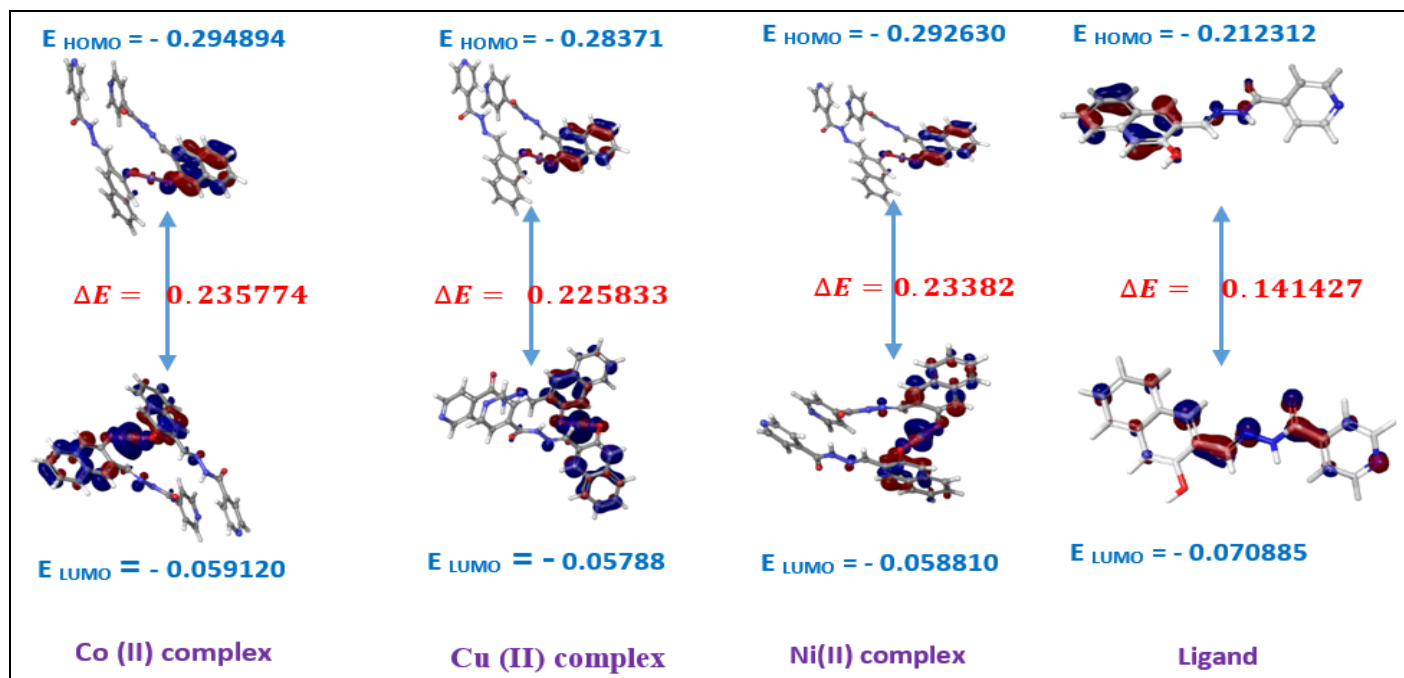


Fig 24 FMO Images of Synthesized Ligand and Metal Complexes.

Table 6 Quantum Chemical Parameters of Ligand and its Metal Chelates.

Electronic parameters	Schiff baseLigand	Cu (II) Complex	Co (II) complex	Ni (II) complex
$E_{HOMO}$ (eV)	-0.212312	-0.28371	-0.294894	-0.292630
$E_{LUMO}$ (eV)	-0.070885	-0.05788	-0.059120	-0.058810
$\Delta E = E_{HOMO} - E_{LUMO}$ (eV)	0.14142	0.225833	0.235774	0.23382

## VII. CONCLUSION

This study established that the newly synthesized Cu(II), Co(II), and Ni(II) coordination complexes incorporating a Schiff base ligand were comprehensively elucidated by an array of analytical and spectroscopic methodologies. The interactions of these complexes with calf thymus DNA (CT-DNA) were interrogated via electronic absorption spectroscopy, viscometric analyses, and thermal denaturation assays. The experimental findings demonstrated that all complexes associate with duplex DNA, exhibiting intrinsic binding constants of  $1.83 \times 10^6$  M $^{-1}$ ,  $4.43 \times 10^6$  M $^{-1}$ , and  $2.73 \times 10^6$  M $^{-1}$  for the Cu(II), Co(II), and Ni(II) derivatives, respectively. A progressive increase in the relative viscosity of CT-DNA was observed with incremental additions of the complexes. Thermal denaturation profiles further corroborated the formation of stable DNA–metal complex adducts. Nuclease-mimetic (DNA cleavage) assays employing pUC18 plasmid DNA indicated that all metal complexes display pronounced DNA scission activity. Additionally, in silico molecular docking simulations conducted using HEX 8.0 software identified intercalative insertion as the predominant binding modality and revealed differential DNA-binding energies among the

complexes. Frontier molecular orbital characteristics (HOMO–LUMO distributions and energy gaps) were further interrogated using density functional theory (DFT). Collectively, the data indicate that the metal center, the electronic nature of the ligand substituents, and the azomethine (C=N) moiety in the ligand framework synergistically facilitate the development of an efficient DNA-responsive probe and likely underpin the observed bioactivity profiles of the free ligand and its corresponding metal chelates.

## ACKNOWLEDGEMENTS

The authors are thankful to the Chairman of the Department of Industrial Chemistry at *in Industrial Chemistry, Sir. M.V. Govt. Science College, Bommanakatte, Bhadravathi*, for providing the laboratory facilities and to the Gandhigram Rural Institute (Deemed to be a university) in Gandhigram, Dindigul District, Tamil Nadu, for performing the spectral characterization.

### ➤ Author's Contributions:

Erushanaik: Methodology, Investigation, Writing – original draft. Prabhakar M C: Methodology, Investigation,

Supervision, Writing, and editing of original draft. Surendranaiak Y: DFT studies.

➤ **Disclosure Statement:**

No potential conflict of interest was reported by the authors.

➤ **Funding:**

The authors reported that there is no funding associated with the work featured in this article.

➤ **Data Availability Statement:**

The authors confirm that the data supporting the findings of this study are available within the article [and/or] its supplementary materials.

## REFERENCES

- [1]. Durmus S, Atahan A, Zengin M. Synthesis, characterization and electrochemical behavior of some Ni (II), Cu (II), Co (II) and Cd (II) complexes of ONS type tridentate Schiff base ligand. *Spectrochim. Acta A*. 2011; 84:1–5.
- [2]. Chowala TN, Desai KR. Synthesis, characterization, antibacterial and DNA binding studies of Mn (II) complex of 3-(2-(2-hydroxy-3-methoxybenzylidene)hydrazinyl) quinoxalin-(1H)-One. *J. Appl. Chem.* 2015; 8:5–10.
- [3]. Khedr AM, Saad FA. Turk, Synthesis, structural characterization, and antimicrobial efficiency of sulfadiazine azo-azomethine dyes and their bi-homonuclear uranyl complexes for chemotherapeutic use. *J. Chem.* 2015; 39:267–80.
- [4]. El-Baradie K, El-Sharkawy R, El-Ghamry H, Sakai K. Synthesis and characterization of Cu (II), Co (II) and Ni (II) complexes of a number of sulfadiazine dyes and their application for wastewater treatment. *Spectrochim. Acta* 2014; 121:180–7.
- [5]. El-Sonbati AZ, Diab MA, Morgan ShM, Abou-Dobara MI, El-Ghettany AA. Synthesis, characterization, theoretical and molecular docking studies of mixed-ligand complexes of Cu (II), Ni (II), Co (II), Mn (II), Cr (III), UO<sub>2</sub>(II) and Cd (II). *J. Mol. Struct.* 2020; 1200:127065.
- [6]. Saad FA, Ghamry HA El, Kassem MA, Khedr AM. Synthesis, characterization for new nanometric VO(II)-Thioacetamide complexes by, spectral, thermal, molecular computations and DNA interaction study beside promising antitumor activity. *J. Inorg. Organomet. Polym. Mater.* 2019; 29:1606–24.
- [7]. Sarkar T, Banerjee S, Hussain A. Significant photocytotoxic effect of an iron (III) complex of a Schiff base ligand derived from vitamin B6 and thiosemicarbazone in visible light. *RSC Adv.* 2015; 5:29276–84.
- [8]. Banerjee S, Dixit A, Maheswaramma K, Maity B, Mukherjee S, Kumar A, Karande A, Chakravarty AR. *J. Chem. Sci.* 2016;128:165–75.
- [9]. El-Sonbati AZ, Diab MA, Morgan ShM, Eldesoky AM, Balboula MZ. Polymer complexes. LXIX. Some divalent metal (II) polymer complexes of potentially bidentate monomer N-[4-(5-methyl-isoxazol-3-ylsulfamoyl)-phenyl]-acrylamide: synthesis, spectroscopic characterization, thermal properties, antimicrobial agents and DNA studies. *Appl. Organomet. Chem.* 2018;32: e4207.
- [10]. Sudhamani CN, Bhojya Naik HS, Ravikumar Naik TR, Prabhakara MC. Synthesis, DNA binding and cleavage studies of Ni (II) complexes with fused aromatic N-containing ligands. *Spectrochim. Acta, Part A* 2009;72:643–7
- [11]. Prakash Naik HR, Bhojya Naik HS, Ravikumar Naik TR, Raja Naika H, Goutham Chandra K, Mahmood R, Khadeer Ahamed BM. Synthesis of novel benzo[h] quinolines: wound healing, antibacterial, DNA binding and in vitro antioxidant activity. *Eur. J. Med. Chem.* 2009; 44:981–9.
- [12]. Ravikumar Naik TR, Bhojya Naik HS, Prakash Naik HR, Bindu PJ, Harish BG, Krishna V. Synthesis, DNA binding, docking and photocleavage studies of novel benzo[b] [1,8] naphthyridines. *Med. Chem.* 2009; 5:411–8.
- [13]. Rajaraman D, Sundararajan G, Loganath NK, Krishnasamy K. Synthesis, molecular structure, DFT studies and antimicrobial activities of some novel 3-(1-(3,4-dimethoxy phenethyl)-4,5-diphenyl-1H-imidazole-2-yl)-1H-indole derivatives and its molecular docking studies. *J. Mol. Struct.* 2017; 1127:597–610.
- [14]. Bheemarasetti M, Palakuri K, Raj S, Saudagar P, Gandamalla D, Reddy Yellu N, Kotha LR. Novel Schiff base chelates: synthesis, characterization, DNA binding, DNA cleavage and molecular docking studies. *J. Iran. Chem. Soc.* 2018; 15:1377–89.
- [15]. Prabhakara MC, Bhojya Naik HS, Krishna V, Kumaraswamy HM. Binding and oxidative cleavage studies of DNA by mixed ligand Co (III) and Ni (II) complexes of quinolo [3,2-b] Benzodiazepine and 1,10-phenanthroline. *Nucleos Nucleot. Nucleic Acids* 2007; 26:459–71.
- [16]. Dholayika PP, Patel MN. Synth. React. Inorg. Preparation, characterization, and antimicrobial activities of some mixed-ligand complexes of Mn (II), Co (II), Ni (II), Cu (II), and Cd (II) with monobasic bidentate (ON) schiff base and neutral bidentate (NN) LigandsMet-org. *Nano-Chem.* 2004;34:383–95.
- [17]. El-Sonbati AZ, Diab MA, El-Binary AA, Abou-Dobara MI, Seyam HA. Molecular docking, DNA binding, thermal studies and antimicrobial activities of Schiff base complexes. *J. Mol. Liq.* 2016; 218:434–56.
- [18]. Tursunov MA, Avezov KG, Umarov BB, Parpiev NA. 1H NMR spectra and crystal structure of the nickel (II) complex with ethyl 5,5-dimethyl-2,4-dioxohexanoate arylhydrazones. *Russ. J. Coord. Chem.* 2017; 43:93–6.
- [19]. Kirthan BR, Prabhakara MC, Bhojya Naik HS, Amith Nayak PH, Indrajith Naik E. Synthesis, characterization, DNA interaction and anti-bacterial studies of Cu(ii), Co(ii) and Ni(ii) chelates containing azo-dye ligand. *Chem. Data Col.* 2020;29: 100506.

[20]. Manjuraj T, Krishnamurthy G, Bodke YD, Bhojya Naik HS, Anil Kumar HS. Synthesis, XRD, thermal, spectroscopic studies and biological evaluation of Co (II), Ni (II) Cu (II) chelates derived from 2-benzimidazole. *J. Mol. Struct.* 2018;1171: 481–7.

[21]. Dholakiya PP, Patel MN. Synthesis, spectroscopic studies, and antimicrobial activity of Mn (II), Co (II), Ni (II), Cu (II), and Cd (II) complexes with bidentate schiff bases and 2,20 -bipyridylamine. *Synth. React. Inorg. Met. Org. Chem.* 2002; 32:753–62.

[22]. Dholakiya PP, Patel MN. Preparation, magnetic, spectral, and biocidal studies of some transition chelates with 3,5-dibromosalicylideneaniline and neutral bidentate ligands, syn. *React. Inorg. Met. Org. Nano-Met. Chem.* 2002; 32:819–29.

[23]. Peker E, Serin S. Synthesis and characterization of some cobalt (II), copper (II), and nickel (II) complexes with new schiff bases from the reaction of p-amino azobenzene with salicylaldehyde synth. *React. Inorg. Met. -Org. Chem.* 2004; 34:859.

[24]. Amith Nayak PH, Bhojya Naik HS, Viswanath R, Kirthan BR. Green light emitting fluorescent [Zn (II) (Schiff base)] complexes as electroluminescent material in organic light emitting diodes. *J. Phys. Chem. Solid.* 2021; 159:110288.

[25]. Nagaraja O, Bodke YD, Pushpavathi I, Ravi Kumar S. Synthesis, characterization and biological investigations of potentially bioactive heterocyclic compounds containing 4-hydroxy coumarin. *Helion* 2020; 6:04245.

[26]. Amith Nayak PH, Bhojya Naik HS, Teja HB, Kirthan BR, Viswanath R. Synthesis and opto-electronic properties of green light emitting metal Schiff base complexes. *Mol. Cryst. Liq. Cryst.* 2021;1–7.

[27]. Prabhakara MC, Basavaraju B, Bhojya Naik HS. Co (III) and Ni (II) complexes containing bioactive ligands: synthesis, DNA binding, and photocleavage studies. *Bioinorgan. Chem. Appl.* 2007;7–13.

[28]. El-Sonbati AZ, Diab MA, El-Binary AA, Abou-Dobara MI, Seyam HA. Molecular docking, DNA binding, thermal studies and antimicrobial activities of Schiff base complexes. *J. Mol. Liq.* 2016; 218:434–56.

[29]. Sangeetha Gowda KR, Bhojya Naik HS, Vinay Kumar B, Sudhamani CN, Sudeep HV, Ravikumar Naik TR, Krishnamurthy G. Synthesis, antimicrobial, DNA-binding and photo nuclease studies of Cobalt (III) and Nickel (II) Schiff base complexes. *Spec. Chim. Acta Part A*. 2013; 105:229–37.

[30]. Boubakri L, Chakchouk-Mtib A, Al-Ayed Abdullah, Mansour L, Abutaha N, Harrath AH, Mellouli L, Ozdemir I, Yasar S, Hamdi N. Ru (II)-N-heterocyclic carbene complexes: synthesis, characterization, transfer hydrogenation reactions and biological determination. *RSC Adv.* 2019; 9:34406–20.

[31]. Pradeepa SM, Bhojya Naik HS, Vinay Kumar B, Priyadarsini KI, Barik A, Ravikumar Naik TR. Cobalt (II), Nickel (II) and Copper (II) complexes of a tetradeятate Schiff base as photosensitizers: quantum yield of  $\text{IO}_2$  generation and its promising role in anti-tumor activity. *Spec. Chim. Acta Part A: Mol. Biomol. Spec.* 2013; 101:132–9.

[32]. Vinay Kumar B, Bhojya Naik HS, Girija D, Sharatha N, Pradeepa SM, Joy Hoskeri H, Prabhakara MC. Synthesis, DNA-binding, DNA-photo nuclease profiling and antimicrobial activity of novel tetra-aza macrocyclic Ni (II), Co (II) and Cu (II) complexes constrained by thiadiazole. *Spec. Chim. Acta Part A*. 2012; 94:192–9.

[33]. Sudhamani CN, Bhojya Naik HS, Sangeetha Gowda KR, Giridhar M, Girija D, Prashanth Kumar PN, Synthesis. DNA interactions and antibacterial PDT of Cu (II) complexes of phenanthroline based photosensitizers via singlet oxygen generation. *Spec. Chim. Acta Part A*. 2015; 138:780–8.

[34]. Huang X, Sun W, Cheng Z, Chen M, Li X, Wang J, Sheng G, Gong W, Wang Y. Structural basis for two metal-ion catalysis of DNA cleavage by Cas12i2. *Nat. Commun.* 2020; 11:5241.

[35]. Kirthan BR, Prabhakara MC, Bhojyanaik HS, Viswanath R, Amith Nayak PH. Optoelectronic, photocatalytic and biological studies of mixed ligand Cd (II) complex and its fabricated CdO nanoparticles. *J. Mol. Struct.* 2021; 1244:130917.

[36]. Huang X, Sun W, Cheng Z, Chen M, Li X, Wang J, Sheng G, Gong W, Wang Y. Structural basis for two metal-ion catalysis of DNA cleavage by Cas12i2. *Nat. Commun.* 2020; 11:5241.

[37]. Jayaseelan P, Prasad S, Vedanayaki S, Rajavel R. Synthesis, characterization, antimicrobial, DNA binding and cleavage studies of Schiff base chelates. *Arab. J. Chem.* 2016; 9:668–77.